PERSPECTIVE • OPEN ACCESS

Grand challenges in the design and manufacture of vascular self-healing

Multifunctional Materials

PERSPECTIVE

Grand challenges in the design and manufacture of vascular self-healing

Isabel P S Qamar[1,2], Nancy R Sottos[3] and Richard S Trask[2]

[1] Computer Science and Artificial Intelligence Laboratory, Massachusetts Institute of Technology, 32 Vassar Street, Cambridge, MA 02139, United States of America
[2] Bristol Composites Institute, Department of Aerospace Engineering, University of Bristol, Queens Building, University Walk, Bristol BS8 1TR, United Kingdom
[3] Beckman Institute for Advanced Science and Technology, University of Illinois at Urbana-Champaign, 405 North Mathews Avenue, Urbana, IL 61801, United States of America

E-mail: ipsqamar@mit.edu

Keywords: self-healing, additive manufacturing, multifunctional materials, grand challenges

OPEN ACCESS

PUBLISHED
27 February 2020

Abstract

This perspective details the grand challenges of designing and manufacturing multifunctional materials to impart autonomous property recovery. The susceptibility of advanced engineering composites to brittle fracture has led to the emergence of self-healing materials. This functionality has been demonstrated in bulk polymers and fibre-reinforced composites; most recently through the addition of vascular networks into the host material. These network systems enable the healing agents to be transported over long distances and provide a means by which both the resin and hardener can be replenished, thus overcoming the inherent limitations of capsule-based systems. To date, vascule fabrication methods include machining, fugitive scaffold processes, a lost-wax process and the vaporisation of sacrificial components, but recent developments in additive manufacturing (AM) technologies have paved the way for more efficient, bio-inspired vascular designs (VDs) to be realised. This perspective reviews the current progress in vascular self-healing and discusses how AM technologies and new design methods can be exploited in order to fabricate networks that are optimised for fluid transport and structural efficiency. The perspective culminates in the discussion of eight grand challenges across three thematic areas: 'VD', 'Healing Chemistry' and 'AM', that are likely to have major breakthroughs and socio/economic impact as these technologies are developed further in the next 10–15 years.

1. Introduction

The engineering components and products of today are expected to be structurally optimised and energy efficient; designers are striving to minimise the environmental footprint whilst maximising the operational performance of the whole system. This philosophy is driving the development and application of advanced polymer materials to all market sectors.

Throughout the life-cycle of these light-weight, energy-efficient engineering systems (typically 25–50 years), it is highly likely that parts will become damaged or possibly degrade. This could be a simple cosmetic scratch, failure of a sub-system or full structural failure of the primary architecture. Therefore, to achieve the designer's intent of maximising the operational performance, there is a fundamental need to design and develop materials with the innate ability to repair without compromising the structural performance, and without human intervention. The goal of this perspective is to review the recent developments in multifunctional vascular self-healing in terms of design and fabrication methodologies and to formulate the grand challenges to facilitate future breakthroughs in the application of self-healing materials.

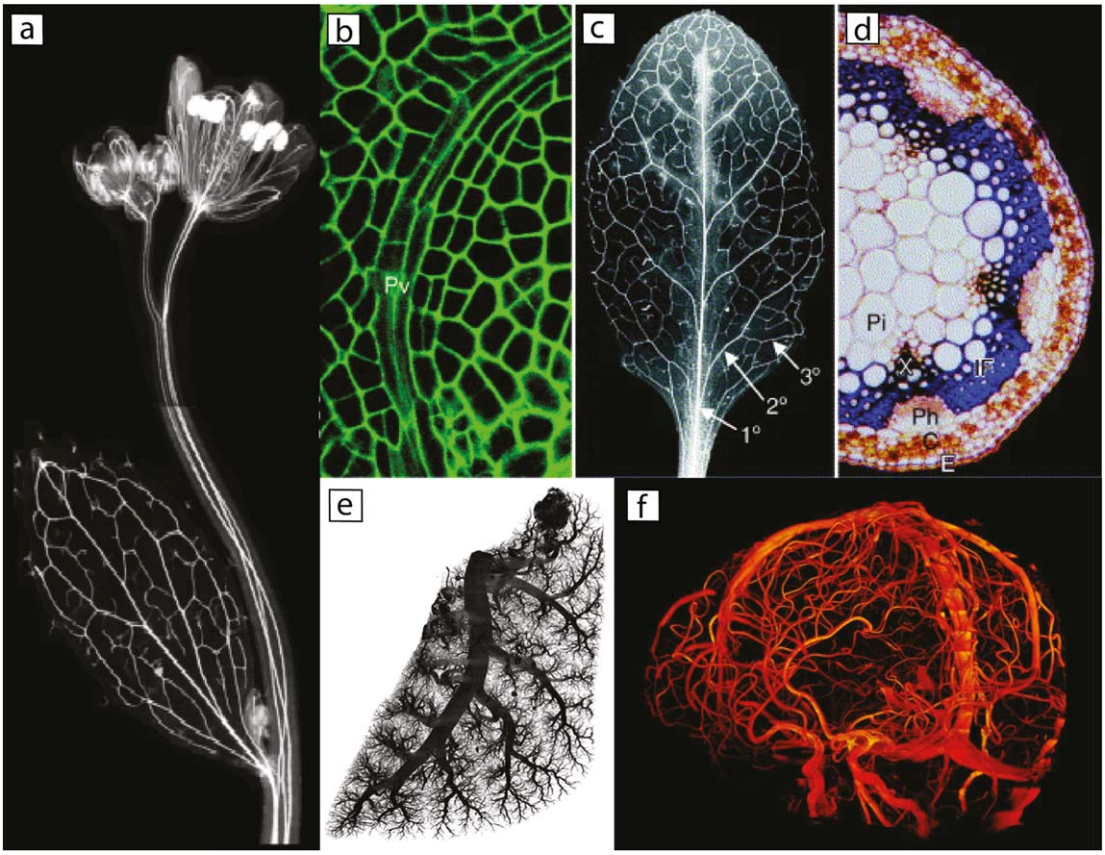

Figure 1. Vascular systems in nature: (a) vascular system in a plant connecting developing flowers, cauline leaves and axillary buds (Reproduced from [26] with permission from the Company of Biologists Ltd. Copyright 1999). Levels of vascular tissue organisation in plants: (b) alignment of cells in a provascular (Pv) strand of a young leaf primordium; (c) the network of vascular strands in an Arabidopsis rosette leaf (1°, primary vein; 2°, secondary vein; 3°, tertiary vein); (d) organ-specific internal organisation of vascular bundles in Arabidopsis stems (C, cortex; E, epidermis; IF, interfascicular fibres; Ph, phloem; Pi, pith; Pv, provascular strand; X, xylem) (Reproduced from [27] with permission from Elsevier. Copyright 2000). (e) Computer-generated projection display of the pulmonary arterial tree within isolated rat lungs (Reproduced from [28] with permission from the authors. Copyright 2005). (f) Cerebral blood vessels in a human brain (Reproduced from [29] with permission from the Centre for Advanced Imaging, University of Queensland, Australia. Copyright 2018).

Self-healing in bulk polymers [1–10], fibre-reinforced composite laminates (FRPs) [11–22] and sandwich cores [23, 24] has already been demonstrated. Of particular interest is the integration of vascular networks that allow healing agents to be delivered from an external source to damage sites throughout a structure, with the possibility of repeated healing by enabling the healing agents to be continually replenished. Several challenges, however, still remain. Firstly, the ability to achieve repeated healing has been largely limited by the network architecture which requires fracture in order for the healing agents to secrete out into the damage zone. Typically this leads to thrombosis of the network, thus preventing any further flow of healing agent. Secondly, the scale-up of the networks also requires addressing; at present, damage can only be repaired in relatively close proximity to the vascules. Finally, integration of the networks into structural composites still needs investigation in order to ensure minimum disruption to the host material [25].

We may be able to address some of these challenges by looking to nature, where vasculature plays a critical role in enabling life support functions, such as distributing nutrients around a plant for photosynthesis or transporting blood cells to repair damage to the human body (figure 1). The architecture of these systems has evolved to transport fluid as efficiently as possible. While such systems are yet to be realised in self-healing materials, additive manufacturing (AM) holds promise for creating biologically-inspired designs that could result in higher degrees of healing efficiency with a reduced infusion time.

In this article, we focus on the developments in vascular self-healing polymers and composites. We begin by describing the current methods for vascule fabrication (machining, fugitive scaffold processes, the 'lost-wax' process and the vaporisation of sacrificial components (VaSC)) and discuss their limitations. We then review the literature on biological vascular systems and discuss how synthetic vascular networks that more closely represent those found in nature, can be fabricated by exploiting the advances in AM. Finally, this perspective concludes with a discussion on the future direction of multifunctional self-healing and how this will change our design philosophy in the next 5–10 years.

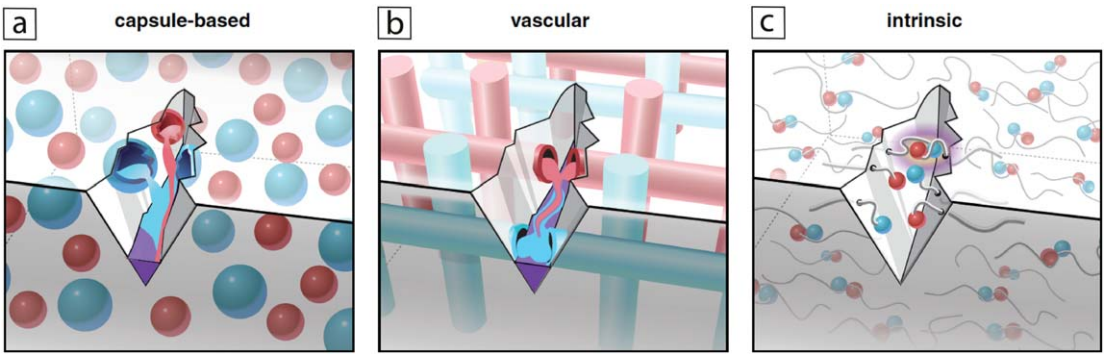

Figure 2. Approaches to self-healing of materials: (a) capsule-based, (b) vascular, (c) intrinsic (Reproduced from [30] with permission from Annual Reviews, Inc. Copyright 2010).

2. Vascular self-healing systems

The three main approaches to self-healing, namely microcapsular, intrinsic and vascular (figure 2), differ by their means of introducing healing functionality, which consequently influences the healable damage volume, repeatability and rate of healing. Intrinsic self-healing relies on the material having some inherent ability to repair itself. This type of healing is accomplished through a number of methods including thermally reversible reactions, hydrogen bonding, ionomeric coupling, a dispersed meltable thermoplastic phase or molecular diffusion. High healing efficiencies and multiple healing events have been achieved using intrinsic systems; however, intrinsic re-bonding requires close proximity of the damaged surfaces, thus limiting healing to small damage volumes [30–32].

The first significant breakthrough and, perhaps, the most explored route to achieving self-healing of polymeric materials, is through a microcapsule-based approach. In the initial landmark paper published by White *et al* in 2001 [33], a dicyclopentadiene (DCPD) monomer was encapsulated within a urea-formaldehyde (UF) shell to form microspheres of 50–200 μm in diameter. 10 wt% of these microcapsules, along with 2.5 wt% Grubbs' catalyst (a highly-active, Ruthenium-based transition metal catalyst), were then embedded within an epoxy matrix. When a crack propagated through the structure and ruptured open a microcapsule (figure 3(a)), the contained healing agent was released onto the fracture plane and polymerised on contact with the Grubbs' catalyst through a ring-opening metathesis polymerisation reaction, bonding the crack faces together and recovering fracture properties. Figure 3(b) shows that on the retesting of tapered double cantilever beam (TDCB) specimens in mode I, up to 75% recovery in fracture toughness was achieved. Further research has since been conducted to improve the efficiency of this self-healing system [2, 12, 34], including investigations into different healing chemistries (HCs) [35–39] and the potential of achieving self-activated healing in fibre-reinforced composite materials [38, 40, 41]. However, although microcapsules can easily be incorporated within a polymer-based material and can achieve high healing efficiencies in small to moderate damage volumes [30], during a healing event, fracture of the microcapsule is required which leads to local depletion of the healing agent and potential voids where it was once stored. As a result, this self-healing approach is limited locally to a single healing event as long-range transport of the healing agent is not possible [25].

Integrating vascular networks into materials provides an effective delivery mechanism for the healing agents to reach the damage site, transporting them over long distances and a means by which both resin and hardener can be replenished. This overcomes the main limitation associated with encapsulated systems and enables the possibility of multiple healing events. Several techniques have been exploited to create vascular networks within a range of materials, including sandwich cores [23, 24], bulk polymers [1–10] and FRPs [11–22]. Each of these methods, discussed in turn below, has been used to achieve successful reinstatement of mechanical properties and, in some cases, to address multiple healing events.

2.1. Subtractive manufacturing

Microvascular self-healing networks have been shown to effectively heal impact damage in sandwich structures, specifically skin/core debonding, and offer complete recovery of flexural failure mode and load. Williams *et al* [23, 24] constructed vascularised sandwich cores by embedding commercially available PVC tubing with a 1.5 mm bore, within closed-cell foam. Holes were drilled through the foam core and into the PVC tubes to form vertical risers for the fluid to reach the skin/core interface (figure 4(a)). E-glass epoxy laminates were then adhered to either side of the core and the resulting sandwich panel was cured, following which, miniature barbed tubing connecters were attached to the ends of the PVC tubing to allow an external reservoir to be connected.

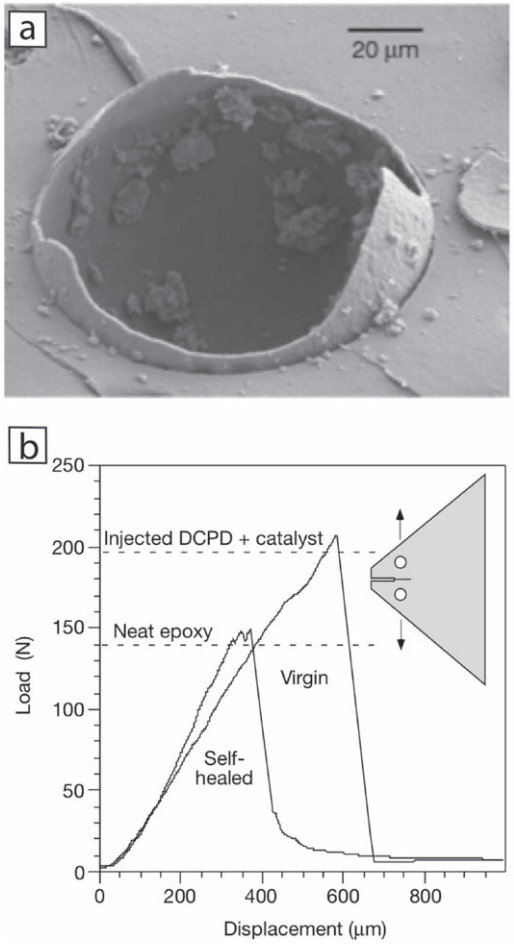

Figure 3. (a) A scanning electron microscope (SEM) image of a broken microcapsule embedded within a polymer matrix; (b) healing efficiency of TDCB specimens (Reproduced from [33] with permission from the authors. Copyright 2001).

The channels ruptured on impact, allowing the healing agents to infuse the damaged region before curing (figure 4(b)). Four-point bend tests confirmed the complete restoration of mechanical performance and, by filling the channels with alternating hardener and resin, a fully autonomous healing system was achieved when both networks were successfully breached. Further optimisation of the design of this self-healing sandwich system has since been carried out [43], including discussions into reliability optimisation [44]. Repair of polyurethane foam cores has also been demonstrated, made possible by the machining of approximately 1 mm diameter, longitudinal channels into the foam to transport the healing agents to the damage site [45].

2.2. Fugitive scaffold processes via novel chemistry

Toohey *et al* [3] designed three-dimensional (3D) microvascular networks to repair cracks in an epoxy coating. The interconnected networks, located within the epoxy matrix substrate, were fabricated using direct-write assembly (DWA), a technique that was refined by Therriault *et al* [4, 5]. Here, scaffolds were created by depositing fugitive ink; the scaffolds were then infiltrated with epoxy, the epoxy cured and the scaffolds removed by applying heat and vacuum, resulting in a series of 200 μm hollow channels. An epoxy coating containing particles of Grubbs' catalyst was deposited on the substrate and the networks were filled with DCPD healing agent. Following this, the samples were loaded in four-point bend to initiate the cracks (the presence of which was detected by an acoustic-emission signal), which then propagated towards the channel openings due to a local reduction in beam stiffness. The healing agent infused and healed the damage site through capillary action without the need for external pressure (figure 5(a)), and the resin system was then cured at 25 °C for 12 h. This process was repeated until no further healing events occurred. A peak load recovery of 70% was noted after the second event; however, the concentration of catalyst present in the coating ultimately dictated the number of possible healing cycles, with a maximum of 7 being achieved at 10 wt% catalyst due to its eventual depletion.

In an attempt to overcome this limitation, a further study by Toohey *et al* [6] replaced the resin/catalyst system with a two-part epoxy-based HC. Four independent networks of 300 μm in diameter that contained alternating resin and hardener were fabricated, as opposed to a single network delivering only monomer to the

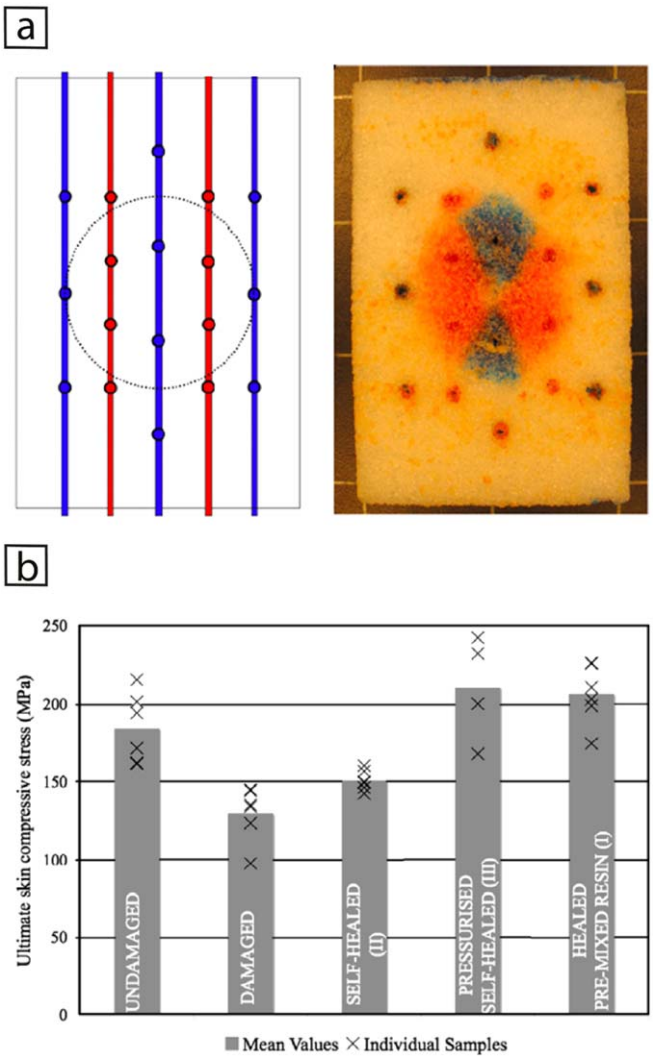

Figure 4. (a) Healing of a disbonded skin-core interface using alternating channels of resin and hardener that are delivered from an external reservoir (Reproduced from [42] with permission from IOP Publishing, Ltd. Copyright 2012); (b) edgewise compression strength for undamaged and damaged samples, and samples with different healing schemes (Reproduced from [24] with permission from Elsevier. Copyright 2008).

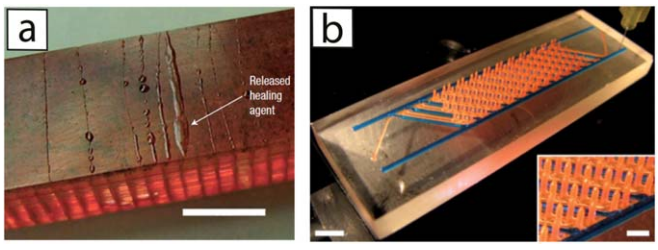

Figure 5. (a) Vascular self-healing structure showing excess healing agent on the surface of the coating after initial crack formation (Reproduced from [3] with permission from the authors. Copyright 2007); (b) interpenetrating networks created via direct-write assembly of wax (orange)- and pluronic (blue)-based fugitive inks (scale bar, 5 mm, inset scale bar, 1 mm) (Reproduced from [7] with permission from John Wiley and Sons. Copyright 2009).

crack site, thus eliminating the need for a catalyst to be embedded in the coating. After cracking, specimens were subjected to cyclic loading to promote mixing of the two components and cured at 30 °C for 48 h. The coatings were repeatedly cracked and healed until no further healing could be achieved, leading to 16 successful healing cycles out of 23. Healing was ultimately limited by a build-up of polymerised material above the channels and in the crack plane, which inhibited further flow and mixing of the two healing components.

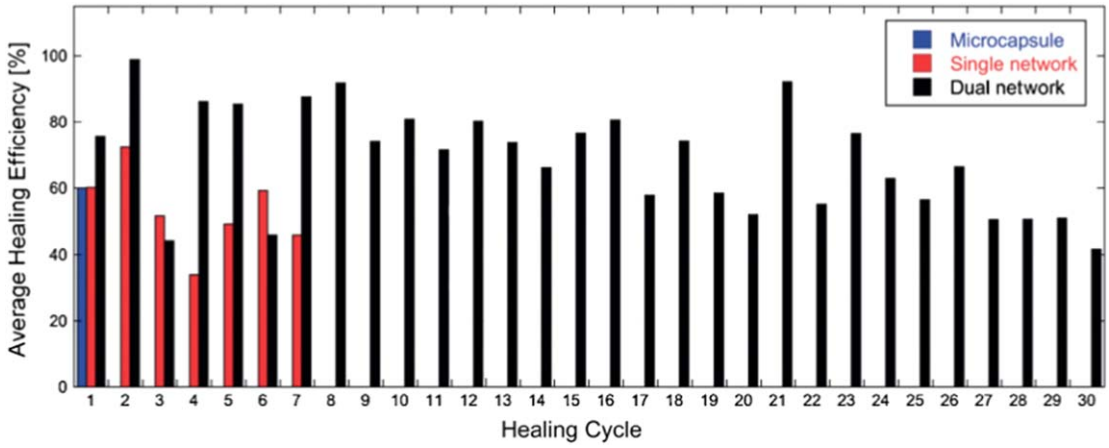

Figure 6. Average healing efficiency for three-dimensional interpenetrating networks (dual) [7] compared with the microcapsule data from White *et al* [33] and the single-network systems investigated by Toohey *et al* [3] (Reproduced from [7] with permission from John Wiley and Sons. Copyright 2009).

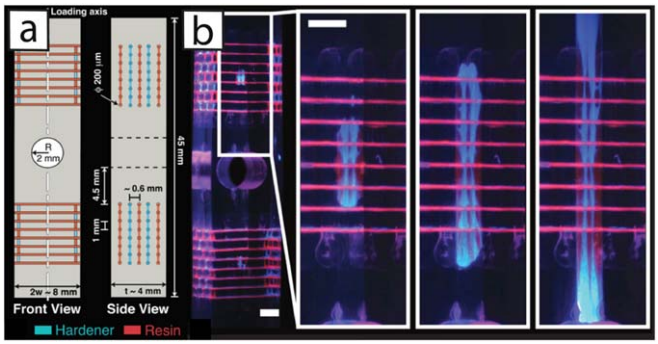

Figure 7. (a) Microvascular DCDC sample geometry (not to scale); (b) diffusion of healing agents into the crack plane (scale bars, 2 mm) (Reproduced from [9] with permission from John Wiley and Sons. Copyright 2010).

Improvements in direct-ink writing (DIW) allowed Hansen *et al* [7] to modify the network architecture and introduce 3D interpenetrating networks (figure 5(b)). Using the same test methodology as implemented by Toohey *et al* [3, 6], healing was achieved for a total of 30 sequential cycles. A comparison with previous healing studies is shown in figure 6, illustrating the significant improvement in number of achievable healing cycles. As the number of cycles increased, the proportion of unsuccessful healing cycles also increased, from 0.25% up to 0.46% for the last few cycles. Introducing an additional, third, interpenetrating network that provided a means to circulate a temperature-controlled fluid by allowing for *in situ* thermal regulation, reduced the healing time by an order of magnitude, from 48 h at 30°C to only 1 h when the circulating fluid was maintained at 70 °C [8]. The aforementioned studies, however, still required the vascular system to be placed away from the location of damage in order to preserve the integrity of the network, and for the channels to terminate where the cracks were most likely to occur, which consequently requires prior knowledge of the probability of damage throughout a structure. Further advances in microvascular fabrication through DIW have since been made with the introduction of omnidirectional printing by Wu *et al* [46]; a technique that provides greater design freedom and eliminates the need for the layer-wise patterning that was demonstrated by Hansen *et al* [7, 8]. However, and critically for advanced materials, due to the fragility of the fugitive wax scaffolds, they are unable to survive composites manufacturing.

Hamilton *et al* [9] demonstrated how DIW could be used to create vascular networks that would permit healing of bulk polymer material, rather than solely the repair of cracks at the skin-core interface. Here, DIW was employed to create microvascular channels, 200 μm in diameter, within epoxy double cleavage drilled compression (DCDC) specimens. By adopting the sample geometry shown in figure 7(a), they demonstrated that cracks that initiate from the crowns of the central hole during compression and propagate outwards, are more inclined to grow in a stable manner and to arrest prior to failure of the entire specimen [1, 47]. The networks contained alternating epoxy resin and hardener throughout the thickness of the sample; each

component being isolated until the crack breached both a resin- and hardener-filled microchannel, and the two components were able to infuse into the crack plane under capillary action and mix (figure 7(b)). This process was repeated and in some cases as many as 13 successful healing cycles occurred. Once again, however, the healing efficiency and number of healed samples decreased with subsequent healing cycles. An examination of the fracture plane indicated that a blockage of the channels caused by a film of polymerised material in the crack plane, which increased in size after each cycle, prevented the healing agents from fully covering the crack plane in subsequent cycles.

Hamilton *et al* [10] later improved this system by introducing an active pumping regime to deliver the healing agents to the crack region under pressure and to promote mixing. By pumping resin and hardener in an alternating sequence, a significant improvement in healing efficiencies and number of cycles was achieved when compared with the previous study [9] that relied upon capillary forces to transport the fluids, with a maximum of almost 100% fracture toughness recovery for 15 cycles. In addition, the total volume of vasculature required for successful healing was significantly reduced due to the improved degree of mixing through the crack site.

2.3. Fugitive vascules via the 'lost-wax' process

The previous studies have shown that incorporating vascular networks into bulk polymer materials has minimal impact on the material properties as the polymer can easily form around the inclusion. However, embedding vasculature into a fibre-reinforced composite laminate poses a significant challenge due to the presence of fibre reinforcement, which can easily be disrupted by the inclusion of any self-healing body and potentially compromise its mechanical properties.

Several studies have examined the effects of including a series of hollow channels within fibre-reinforced composite laminates via a 'lost-wax'-type process. Kousourakis *et al* [48, 49] examined the effect of both inserting hollow glass tubes into the mid-plane of a composite laminate and inserting silicone tubing into the laminate that was removed after cure. They noted that the silicone tended to compress and form an ellipse as a result of the applied pressure during the laminate curing cycle. Fibre waviness and resin rich pockets were inclined to form around the vascules, increasing in size with vascular diameter. Under mode I crack propagation, the microchannels caused an increase in fracture toughness of the host laminate when oriented transversely to the direction of crack propagation, which was attributed to a crack blunting mechanism for the empty channels and crack deflection for the hollow fibres. Larger channels also had a more pronounced detrimental effect on tensile and compressive strengths of the laminate.

Trask *et al* [50] fabricated a vascular network within a carbon-fibre laminate using low melting temperature (LMT) solder wire that was placed at the centreline of the stacked laminate. Post-laminate cure, the LMT wire was removed by heating to 190°C for 2 h under vacuum, leaving a hollow channel within the prepreg plies. This was carried out for varying channel alignments (0°, 45°, 90°) with respect to the fibre orientation. Only a slight degree of fibre waviness was observed when the channels were aligned; however, resin-rich pockets and porosity were present when the channels were misaligned. It was also noted, through 10 J impact tests, that transversely-oriented channels caused an increase in damage area and resulted in degradation in pre- and post-impact strength.

Another method for creating vascules was demonstrated by Huang *et al* [51] and Norris *et al* [19, 20] whereby PTFE-coated, high melting temperature steel wires were inserted into the laminate and pulled out after cure, leaving behind hollow channels. Norris *et al* [19, 20] then went on to explore how this could add self-healing functionality into a structure. They determined that placing vascules (formed from 0.55 mm diameter steel wire), oriented transverse to the fibre direction, into a cut recess in the mid-plane, as opposed to nesting in between the central plies, minimised the formation of large resin pockets and fibre waviness (figure 8), leading to more controlled and predictable crack propagation under modes I and II loading conditions, whilst simultaneously ensuring that the crack cleaves open the vascules. In addition, the presence of vascules acted to arrest the crack for a brief period, increasing the modes I and II strain energy release rates, G_I and G_{II} respectively, until the stored energy was great enough for the crack to propagate around the vascule. Those vascules that were aligned with the fibre direction nested comfortably in between the surrounding fibres with minimal impact on modes I and II fracture toughness.

Compression after impact (CAI) tests, employing a 10 J impact event, confirmed that placing fibres in a recess improves vascule-damage connectivity (figure 9), whilst highlighting that vascule orientation is the controlling factor that influences the mechanical performance of the composite structure. As previously noted, vascules oriented off-axis caused an increase in fibre waviness and resin-rich pockets when nested between plies, and termination of fibres when placed in a cut recess. It was also observed that large diameter vascules enhanced vascule-damage connectivity and infusion of healing agent, reducing the required infusion pressures; however, this resulted in a knockdown in mechanical strength of the host laminate. Self-healing trials were carried out by manually injecting a self-healing resin, DGEBA-EPA-DETA (diglycidyl ether of bisphenol A, eicosapentaenoic

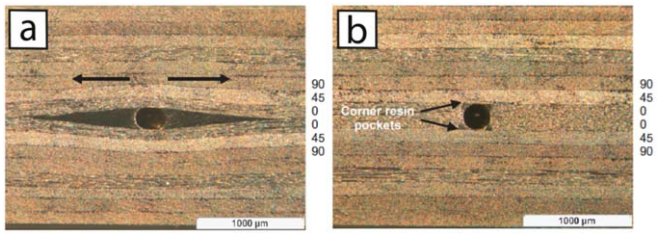

Figure 8. Vascules embedded within a composite laminate transverse to the fibre orientation by inserting (a) in the midplane and (b) within a cut recess (Reproduced from [19] with permission from Elsevier. Copyright 2011).

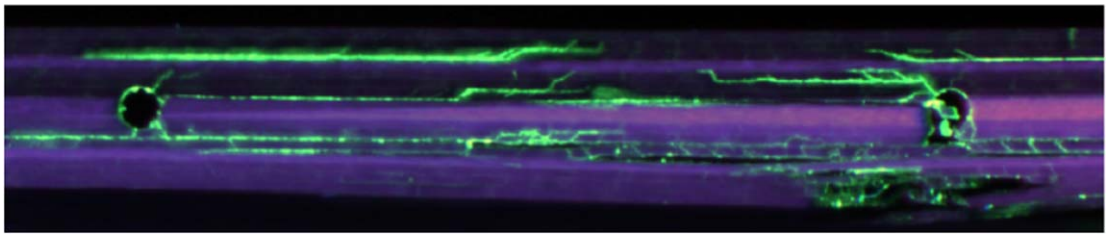

Figure 9. UV dye-aided microscopy of typical damage layout showing interaction of delamination and intra-ply shear cracks (in green) with vascules (Reproduced from [21] with permission from John Wiley and Sons. Copyright 2011).

acid, diethylenetriamine at 100, 25, 12 pph respectively), into the vascules located within the damaged area and leaving the samples to cure for 7 d at room temperature. EPA was employed to reduce the viscosity and allow the resin to infuse more easily. CAI tests on the healed specimens showed recovery of $\geqslant 96\%$ of the post impact compression strength for all vascule configurations, providing evidence that this delivery mechanism can improve the damage tolerance of composite structures [21].

Moving away from a manual system of resin infusion and towards an autonomous stimulus-triggered system, Norris *et al* [42] adapted the structural health monitoring (comparative vacuum monitoring) scheme investigated by Kousourakis *et al* [48, 49] into a self-healing system, whereby one end of a vascule located in the damage region was connected to a low-pressure sensor and the other end sealed. The vascule was pressurised and connected to a controller. On formation of damage and rupture of the vascules, a pressure drop triggered a motor-driven peristaltic pump that circulated a pre-mixed epoxy resin healing agent (low-viscosity RT151, ResinTech) from an external reservoir to a neighbouring vascule, delivering the healing agent to a damage zone for a time period of 5 min. An alternative system was also investigated in which resin was circulated throughout the impact event for 5 min. The result was a recovery of an average of 94% of the undamaged compression strength for the stimulus-triggered system and 100% for the circulatory system. It was proposed that the presence of healing agents circulating in the vascules during the impact event may have affected the formation of damage and infusion of resin into the region.

In an effort to understand how vasculature affects other damage modes, such as delamination, Luterbacher *et al* [52] studied the impact of including hollow vascules at the $0^\circ/90^\circ$ interface within cross-ply laminates, on static tensile properties and fatigue performance. The sparse vasculature had a negligible effect on the performance of the laminate under tensile static and fatigue loading. The authors noted that a reduction in stiffness and strength occurred when loading samples in tension, due to matrix cracks that formed within the 90° layers. A recovery of 75% of the initial failure strength was achieved for samples that were healed using an injection of RT151, a low viscosity epoxy resin. Under fatigue conditions, however, the damage re-opened within the first 2500 cycles, leading to a rapid loss in stiffness which was linked to the poor mechanical performance of the resin system. Nevertheless, the potential for repairing transverse matrix damage through embedded hollow vasculature has been confirmed.

2.4. Vaporisation of sacrificial components (VaSC)

Previous techniques have shown the ability to create simple 1D and 2D vasculature within fibre-reinforced composites and 3D vasculature within neat polymers. Forming and embedding 3D vasculature into fibre-reinforced composites, however, particularly on a large scale, is limited. To address this, a new, highly tailorable approach has recently been developed whereby sacrificial polylactide (PLA) fibres that have been treated with a tin oxalate (SnOx) catalyst, which acts to accelerate thermal decomposition, are woven into 3D woven carbon or

glass preforms and infiltrated with epoxy. On heating above 200 °C after the laminate curing cycle has completed, the PLA fibre vaporises, leaving a hollow 3D vascular network through the composite. These channels can then be used to transport healing agents to a region of damage. As the sacrificial fibres replace a proportion of the preform fibres, disruption to the architecture of the laminate is minimised [53, 54].

Patrick *et al* [22] carried out self-healing trials on woven E-glass/epoxy double cantilever beam (DCB) specimens that contained channels stitched into the fabric and removed after laminate cure, through the VaSC process, in isolated (parallel) and interpenetrating (herringbone) arrangements, as shown in figures 10(a) and (b). Networks introduced into the composite via this vaporisation method were deemed to have little impact on the inherent fracture properties. An EPON 8132/EPIKURE 3046 HC was filled into the dual-vascular channels prior to loading. Samples were loaded and as the channels became increasingly breached, healing agents were continually delivered to the crack plane. On reaching a predefined crack length, samples were unloaded and delivery of healing agents was terminated, following which, the samples were cured. In this manner, multiple healing cycles were attained by retesting the previously healed samples under mode I procedures and increasing the total crack length with each subsequent cycle to expose virgin material.

The results of three successive cycles from this study are shown in figure 10(c), where it was observed that an increase in load is required to initiate and propagate the crack after each healing cycle. In addition, the herringbone pattern arrangement offered healing efficiencies in excess of 100% and an improved performance over the parallel pattern, which was attributed to better mixing within the crack plane due to increased interfacial and overlapping fluid boundary layers, confirming the significance of vascular architecture on *in situ* mixing performance. The authors noted that the ability to repeatedly heal damage was heavily reliant on sufficient availability of the reactive fluids, adequate mixing to ensure sufficient polymerisation and the continued availability of healing agents to the fracture plane after a healing cycle. In regions close in proximity to the terminal crack front, only partially polymerised healing agent was evident on the surface of the crack plane, indicating reduced mixing and thus reduced healing efficiencies with increasing healing cycles.

Gergely *et al* [55] have expanded the capabilities of the VaSC process to include an increased level of dimensionality both in and out of a host polymer, from spheres (0D), fibres (1D) and sheets (2D) to 3D printed structures (figure 11), and verified the viability of this process to transport fluid through flow rate tests.

2.5. Current limitations in vascular self-healing

The healing capabilities of the three predominant healing systems have been introduced and discussed. Intrinsic systems have been shown to repair small damage volumes (up to 1.0 mm^3) [30], with the potential to heal at the molecular scale. Microcapsules have been used to achieve high healing efficiencies in small to moderate damage volumes, however, once the microcapsule has fractured, the healing agent becomes locally depleted thus preventing further repair of damage. Healing larger damage volumes has been demonstrated using vascular networks that allow healing agents to be delivered from an external store and continually replenish. As a result, the limit on the possible healable damage size due to the lack of availability of healing agents, such as that which is in place for microcapsular systems, is theoretically removed. Incorporating vascular networks within fibre-reinforced composites, however, remains challenging due to the disruption of fibre architecture that occurs around inclusions, compromising the mechanical performance of the host material. Nevertheless, self-healing of polymer-based materials after a single damage event has successfully been achieved.

At the time of writing, repeated healing utilising vascular systems has been demonstrated; however, the total number of cycles achievable using embedded networks remains limited, and is highly linked to both the vascular fabrication method and the HCs adopted. In the work carried out by Toohey *et al* [3, 6], up to 16 successful healing cycles out of 23 were attained using a DWA process to repair cracks in polymer coatings. Mixing of the two-part resin system in subsequent healing cycles became increasingly inhibited by the build-up of polymerised material from previous cycles, preventing successful repair of further damage. Additional developments in DIW led to an increase in the number of successful healing cycles to 30 [7, 8]. In addition, experiments confirming the ability to attain up to 13 healing cycles within bulk polymer materials were also published by the same research group [9, 10], but in both of these cases, the blockage of channels due to the increasing presence of polymerised material still remained the limiting factor to further repair.

Patrick *et al* [22] achieved repeated healing of delamination within woven fibre-reinforced composites using 3D vascular architecture fabricated via the VaSC process. They noted that the ability to achieve multiple healing cycles was highly dependent on adequate delivery of the healing agents to the damage site, *in situ* mixing to ensure a high degree of polymerisation, and continued availability of healing agents to the fracture plane in subsequent cycles, with network architecture playing a large part in the degree to which these can be achieved. The authors reported data for three consecutive healing cycles for varying network designs, leading to healing efficiencies greater than 100% for herringbone patterns. However, achieving consecutive healing cycles required fracture of virgin material in order to rupture previously undamaged vasculature and allow healing agents to

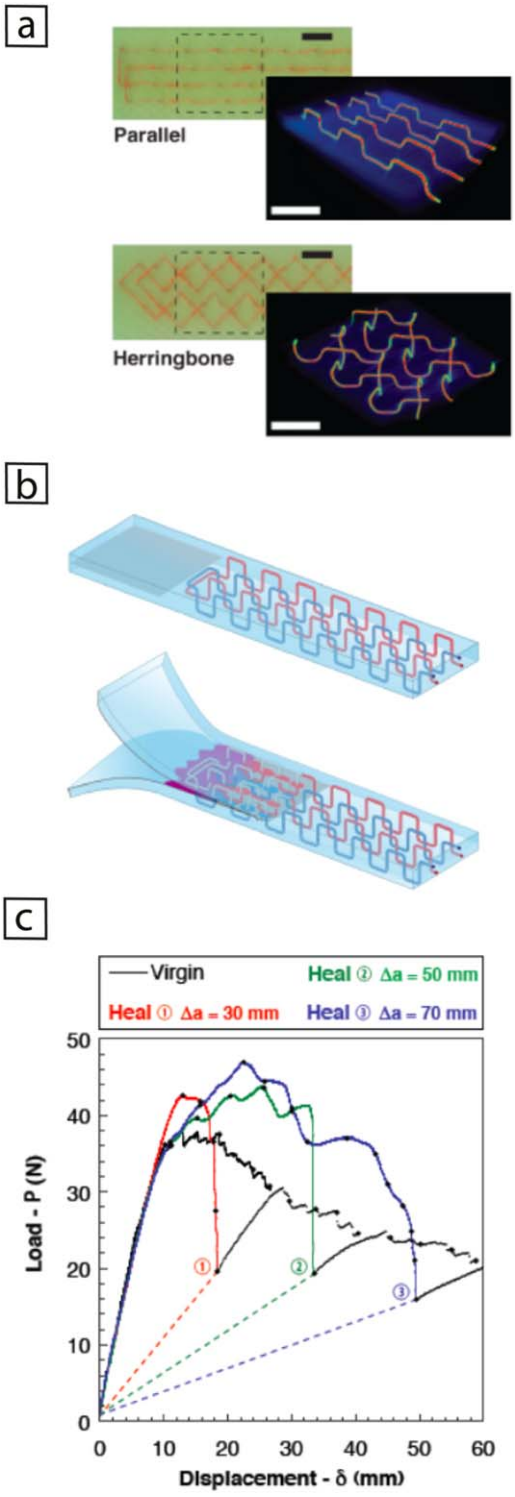

Figure 10. (a) Pre-vascularised, FRP laminate samples displaying sacrificial PLA stitching patterns (scale bars, 10 mm) and corresponding post-vascularised, x-ray computed microtomographic reconstructions of vascular networks (scale bars, 5 mm); (b) schematic of a double cantilever beam (DCB) fracture specimen containing microvasculature; (c) representative load-displacement data for an *in situ* self-healing DCB specimen (herringbone vasculature) subjected to multiple damage cycles (Reproduced from [22] with permission from John Wiley and Sons. Copyright 2014).

continually be delivered to the fracture plane. Therefore, the degree to which repeated healing can be achieved using this technique is dependent upon the number of undamaged vascules left to expose.

These studies have shown that, although self-healing via embedded vasculature can lead to very high healing efficiencies, the ability to achieve multiple healing cycles is limited using current methodologies. This is most commonly due to either rupture of the vascules or blockage of the vascules with polymerised healing agents, both of which prevent fluid from being transported after subsequent damage events. Furthermore, in order to

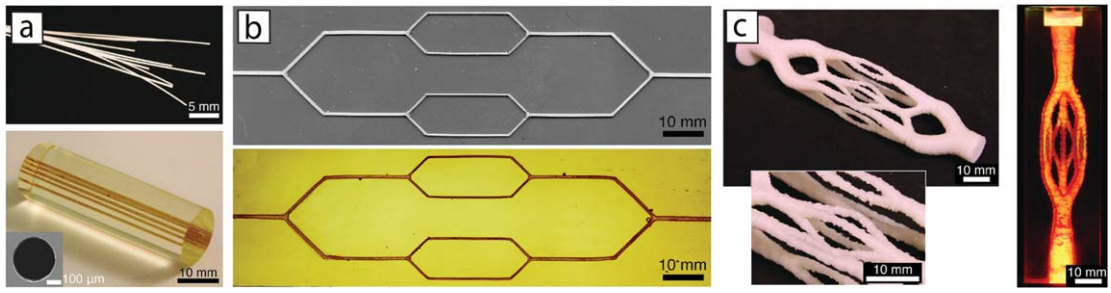

Figure 11. Sacrificial and inverse architectures in (a) 1D, (b) 2D, (c) 3D, fabricated through the VaSC process (Reproduced from [55] with permission from John Wiley and Sons. Copyright 2014).

repair these cracks, the location of damage must be known *a priori* so that the vascules can be placed in positions where they are likely to be breached, indicating the need for a rethink in how self-healing functionality is introduced to a structure. Finally, while additive technologies, such as those used in the VaSC process, have opened up the geometric design freedom that can allow healing to be achieved over a greater damage volume, the optimisation of network design for fluid flow around a self-healing material has still not been well explored.

3. Network design for fluid transport

The design of self-healing vasculature plays a critical role in ensuring the healing agents can rapidly infiltrate the damage site without prior knowledge of where that damage site may be. Another, often conflicting requirement, is that the network imposes as little disruption as possible to the host material, whether that be through minimising the mass of the network and pump required to push the fluid, or through reducing the effect on the surrounding fibre architecture in the case of composite materials. The evolution of AM has made the design and fabrication of highly branched, 3D network structures possible, thereby providing a mechanism for the healing agents to be supplied to a large volume from a single source. It is therefore necessary to understand how the flow may change around these branched networks and how the vascular system can be designed to reduce the global resistance to flow.

The abundance of vascular systems found in nature; from the circulation and breathing systems in mammals to the veins in plants, can provide a valuable source of inspiration for self-healing network design. In this section, an analysis of these systems has been undertaken to identify how they are optimised for fluid transport, with a particular focus on network branching. Following this, various biomimetic and bioinspired approaches to network design found in the literature have been examined in order to recognise any limitations that may occur when implementing these designs into real-life engineered systems.

3.1. Nature's approach to network design

Murray [56] examined the vascular system and cost of blood volume in humans, highlighting that two energy terms contribute to the cost required to maintain blood flow within a vessel: the work required to overcome the viscous drag of the system, and the cost of metabolically maintaining the blood and the vessel tissue involved. To model this, Poiseuille's law [57] that describes the flow of liquids in tubes, was used as an approximation for the pressure loss of laminar flow through a cylindrical tube, and the cost of maintaining the blood was assumed to be directly proportional to the blood volume. The result of these assumptions was to demonstrate that greater pumping power is required for smaller blood vessels due to friction losses, whereas larger blood vessels require greater power to maintain the increased volume of blood. Thus, a minimum power is required for a given blood vessel size and flow.

Based on this analysis, Murray [58] then investigated the principle of minimum work with arterial branching. This led to the deduction of Murray's law that states: where a parent vessel, r_p, splits into daughter vessels, r_d, to minimise power required, the cube of the radius of the parent vessel should equal the sum of the cubes of the radii of the daughter vessels:

$$\sum r_p^3 = \sum r_d^3. \tag{1}$$

Furthermore, Murray derived a law for the angle of the branching of arteries in order to minimise the total energy required, which concluded that the angle of bifurcation of an artery should not be less than 74.9°. Qualitatively, the study agreed with some deductions made by Roux [59] and Hess [60] in that the larger the branch, the greater the deflection in the main artery and the smaller the angle between the branch and direction

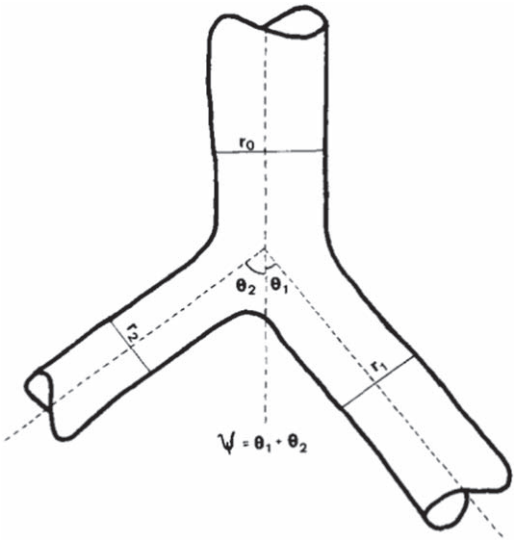

Figure 12. Planar geometry of a bifurcation in the arterial tree, where r_0, r_1 and r_2 are the radii of the parent, major and minor daughters and θ_1 and θ_2 correspond to the major and minor branching angles respectively (ψ is the sum of these angles) (Reproduced from [62] with permission from the Society for Mathematical Biology. Copyright 1982).

of the main stem prior to division (figure 12). Also, branches of equal size make equal angles with the main stem. Uylings [61] extended Murray's model to include both turbulent and laminar flow, shifting the power component in equation (1) from 3 for laminar flow to 2.33 for turbulent flow.

Although the power required for laminar flow depends on the internal diameter (as in Murray's law), the metabolic power requirement depends greatly on the external radius due to the volume of both the vessel and the contained fluid. This indicates that Murray's law is only suitable for vessels with thin walls; however, Sherman [63] noted that the thickness of vessel walls tends to be a linear function of internal radius, as a greater thickness is required to counteract the increased tension in the wall at a greater radius, at a given transmural pressure. The above relationship, therefore, also holds for vessel-wall thickness in this case. Sherman also discussed how Murray's law can be derived for nonliving systems if the vessel material has an initial power cost function that can be amortised over the life of the system.

Sherman *et al* [64] later evaluated the effect of departures from the optimal junction exponent of 3, as derived by Murray's law, on the energy cost. By carrying out an in-depth study of arteriolar trees in cat muscle tissue, they found that the junction exponent was frequently higher than the Murray value of 3, however, the mean junction cost was only 1%–2% and 9% for entire trees. They also suggested that this departure could be minimised by reducing the ratio of parent to daughter diameters in the final arterioral branches. Research investigating optimal lengths for three branches at a junction, based on the branching geometry of the pulmonary artery [65], has also been carried out. On the basis of data garnered by Zamir *et al* [66, 67], Zamir and Brown [68] and Zamir and Medeiros [69], it is now relatively well-known that branching most commonly takes a dichotomous form (i.e. the parent vessel divides into only two daughter vessels) and that the angles and diameters depend largely on the ratio of their diameters [67, 70, 71].

Similar studies to that carried out by Sherman *et al* [64] have been undertaken to assess the validity of Murray's Law, by analysing branching networks found in animals. Taber *et al* [72] studied the developing extra-embryonic blood vessels of 2–4 day-old chick embryos and confirmed that Murray's law holds true even in the early days of life. Zamir *et al* [71] studied the diameter and flow in major branches of the arch of the aorta and found that, at the first few levels of the arterial tree, the relationship between diameter and flow is governed by a 'square law' rather than the classical cube law, whereas the cube law better fits regions of smaller vessels further down the tree.

Plant vasculature tends to take a slightly different form to animal vasculature, in that veins can act to provide a structural role as well as providing a means to transport fluid (figure 13). Price *et al* [73] analysed the branching geometry of 349 leaf vein networks and found that both the radius tapering and parent-to-daughter branch area ratios strongly agreed with predictions obtained using Murray's Law; however, they also noted that, as veins increased in size, the area ratios shifted towards values predicted under an area-preserving relationship (equation (2)) [63, 74], rather than volume-preserving, due a dampened travelling wave from the pulsatile flow. West *et al* [75, 76] showed that conducting tubes must taper to account for variation in total transport path length and, as a result, the resistance and fluid flow per tube are independent of the total path length and plant

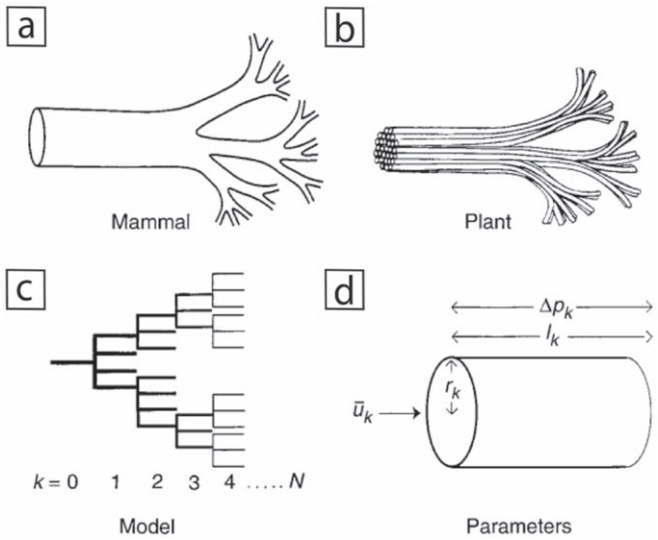

Figure 13. Examples of biological networks: (a) a branched network found in circulatory and respiratory mammalian systems; (b) vessel-bundle vascular systems found in plants; (c) topological representation of such networks, where k specifies the order of the level (0 being the aorta and N, the capillary); (d) parameters of a typical tube at the kth level with length l, radius r, pressure drop p, and flow velocity averaged over the cross section $\bar{u}$ (Reproduced from [75] with permission from The American Association for the Advancement of Science. Copyright 1997).

size. McCulloh *et al* [77, 78] and McCulloh and Sperry [79] determined that plant vessels conform to Murray's law, as long as they only transport water and do not additionally provide structural support to the plant

$$\sum r_p^2 = \sum r_d^2. \tag{2}$$

The comparisons made throughout literature between analytical and computational models and vascular systems found in plants and animals, indicate that Murray's law is a useful starting point in understanding the design of complex vascular systems and how these could be applied to engineered systems.

3.2. Engineering design concepts

Unlike nature, engineering structures have to overcome several implementation challenges, including a lack of technology to support manufacturing at the scale often associated with biological systems, the risks involved with prototyping (i.e. time and cost) and uncertainty with regards to the technological approach, all of which influence the design and manufacture of vascular networks for their intended application.

Engineered materials containing microvascular networks have shown potential as self-healing materials [3, 7], internally cooled materials [53] and constructs for regenerative medicine and bioengineering purposes [80–82], providing a mechanism for the transportation or mixing of fluids [83]. Lim *et al* [84] used a direct write laser technology to fabricate multi-width, multi-depth microfluidic channels within a silicon wafer, that obeyed Murray's law, regardless of exhibiting a non-circular cross-section. They stated that the fluid flow velocities, through channels that changed in accordance with Murray's law, were much less sporadic and may allow for the design of systems with a lower, global resistance to flow, although no experimental data was provided to confirm this.

Emerson *et al* [85] applied Murray's law to a series of arbitrary cross-sections often found in lab-on-a-chip systems. They specifically focused on controlling flow properties within constant-depth square, rectangular and trapezoidal channels, and validated their design through a series of computational fluid dynamics simulations. Their simulations showed excellent agreement with the analysis at low Reynolds numbers, however, above a Reynolds number of 30, the simulations began to deviate due to losses occurring at the 90° bends in the network. Barber and Emerson [86] also noted that throughout the vascular network, the tangential shear stress at the wall remains constant as a direct result of Murray's law. Barber and Emerson [87] later applied these principles into tissue engineering in order to control the shear stress and residence time (relating to the diffusion of nutrients) within the microvascular network.

Constructal theory has often been used as a principle for the design of engineered, flow-based structures, as well as to assist in describing natural flow phenomenon. This law states that '*for a finite-size flow system to persist in time (to live) it must evolve such that it provides greater and greater access to the currents that flow through it*' [88]. Bejan [89] deduced, through constructal theory, that Murray's law, i.e. the optimal ratio between successive tube diameters is $2^{\frac{1}{3}}$ [63], must break down at the smallest volume scale. They established that the optimal ratio

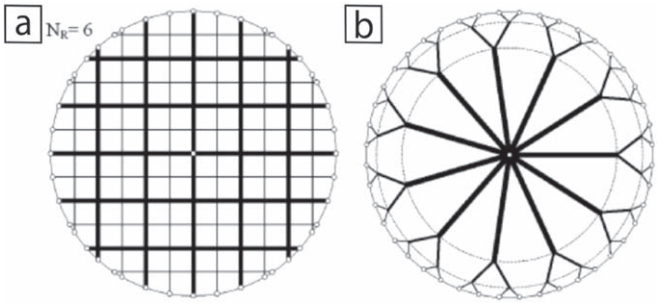

Figure 14. (a) Grid and (b) tree vascular networks filling a circular area, where N_R is a rough measure of the number of grid points in the radial direction (Reproduced from [94] with permission from IOP Publishing, Ltd. Copyright 2007).

between successive tube lengths is also $2^{\frac{1}{3}}$ and showed that the optimisation and construction procedure for a 3D flow network that connects with one point (source or sink), can be repeated to fill the available volume [89, 90]. Analyses on turbulent flow and optimum branching angles also lay in agreement with previous studies [58, 61]. Constructal law has distinctly found its way into smart materials and smart structures, heat transfer and electrokinetic applications, as well as in logistics, biological evolution, art, and business and economics [91]. Here we focus on the way this theory has been used to design vasculature for self-healing polymers and composites.

3.3. Network design for self-healing vasculature

Several researchers have investigated VD strategies for self-healing composite materials. Bejan *et al* [92] considered how to introduce vasculature into a self-healing composite so that healing agents can reach and infiltrate cracks, wherever they may develop, as quickly as possible. To this end, they modelled the crack as a circular defect in a 2D space and suggested that the network should take the form of a grid, rather than a tree (figure 14). Although tree-based networks provide maximum access from an area to a point, in real damage scenarios the positions of the crack or multiple cracks are unknown prior to a damage event and the fluid must have the ability to flow into each and every crack, wherever they may form. They also found that, by considering a network that contains channels of two different diameters, and providing the ratio of the channel diameters is optimised, the global flow resistance of the grid is half of the resistance of a corresponding grid with one channel size [93].

Wang *et al* [94] further explored the idea of incorporating multi-scale grids, i.e. those that have one or more channel sizes, in addition to multi-shape loops and bodies. By increasing the number of optimised channel diameters, the resistance to flow can be minimised. They also found that matching the shape of the network to the shape of the material (i.e. square bodies with square loops and hexagonal bodies with triangular loops), also improves flow access. Finally, they reconfirmed that tree-shaped networks provide better flow access than grid-shaped networks; however, as suggested previously, tree-shaped architectures are only ideal when the locations of the cracks are known in advance. Their study assumed only one crack site needed to be filled, but in reality this is unlikely to be the case. In addition, fully understanding how the healing agents exit a network and enter a crack site still remains a challenge [95].

Williams *et al* [96] presented an analysis that developed expressions for optimum vessel diameter for minimum mass vascular networks, which is often a key design driver in high performance applications. A simple analysis is shown in figure 15(a). They suggested that flow rate has the greatest impact on vascule diameter and that the optimum diameter also depends on whether the network is formed as a tubed system or as a series of channels within the host material (figure 15(b)). They also concluded that, as the mass per unit length of the network increases with increasing numbers of branches, the length of narrower, more numerous vessels should be minimised.

Kim *et al* [97] and Lee *et al* [98] developed asymmetric, vascular architectures on square and rectangular domains with one entry and one exit point that provide fluid to every crack site, considered here as a sub-volume, and examined the coverage ability. The optimal level of performance and vascular architecture to achieve this depends highly on the overall size of the vascular system. They found that a single stream that branched was preferable to several smaller streams that serve clusters of subvolumes, and that the global flow resistance decreases with an increasing number of optimised channel sizes. Kim *et al* [97] noted that larger volumes require a greater level of branching and Cetkin *et al* [99] confirmed this was also the case for turbulent flow. Lorente and Bejan [100] showed that it is possible to ensure fluid can reach every sub-volume of a vascularised material by implementing either the grid system, which is filled with a pressurised healing agent

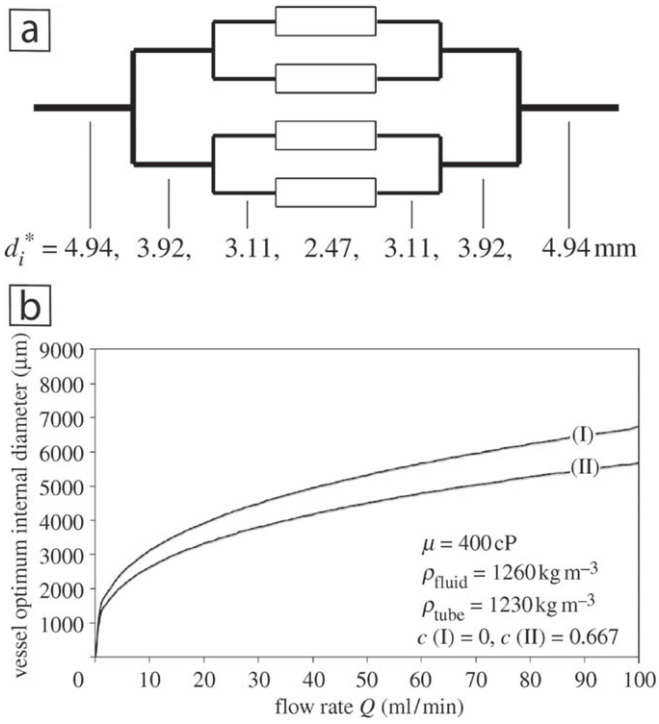

Figure 15. (a) A simple vascular network with optimum vessel diameters, unconstrained by component geometry, where d^* is the optimum vessel diameter; (b) the effect of flow rate on optimum vessel internal diameter, fluid mass only (I) and channel vessel (II), where Q is the volumetric flow rate, μ is the fluid viscosity, ρ_{tube} and ρ_{fluid} are the densities of the tubing material and circulating fluid respectively, and c is a constant of proportionality linking vessel wall thickness with internal diameter, thereby incorporating the strength of the tubing material (Reproduced from [96] with permission from the Royal Society. Copyright 2007).

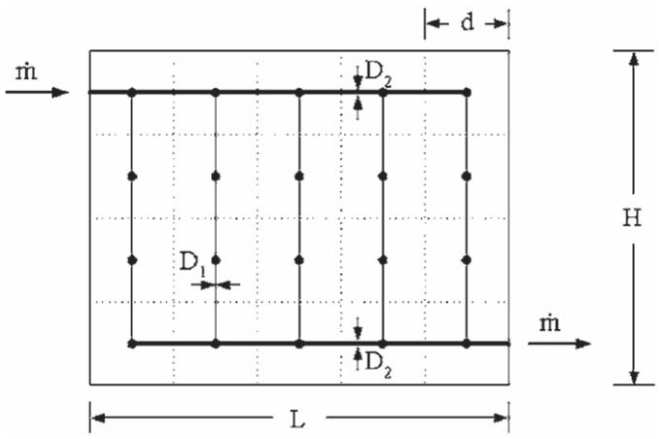

Figure 16. Network design in a rectangular domain containing square elements size d, each supplied with fluid, where H and L are the height and length of the rectangular face of the self-healing composite, D_1 and D_2 are the diameters of the hydraulic trunks of the first and second tree, and $\dot{m}$ is the flow rate through the network (Reproduced from [97] with permission from AIP Publishing. Copyright 2006).

(figure 14), or the canopy-to-canopy system (figure 16) in which the fluid flows at a steady rate through the channels.

Although semi-analytical approaches, such as constructal theory, have been used to establish vascular configurations for optimal coverage; in reality, a large number of design variables exist which may be better suited to gradient-based methods or evolutionary algorithms (EAs). In particular, EAs, such as genetic algorithms (GAs), which are inherently more likely to achieve some global optimisation, use one or more objective function(s) to solve a problem and do so within the entire design space. Aragon *et al* [101] used a multi-objective GA to design 2D and 3D microvascular networks embedded within polymeric materials for self-healing functionality (figure 17(a)). By considering a number of objective functions and constraints, they

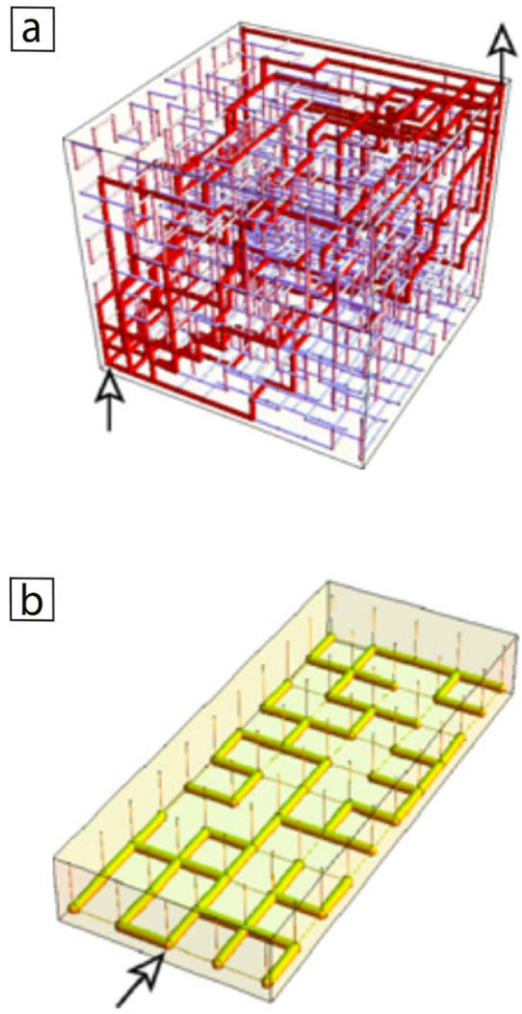

Figure 17. (a) A 3D microvascular network optimised through a genetic algorithm for flow efficiency and reduced volume fraction; (b) 3D network optimisation for self-healing coating experiments, based on achieving uniform distribution of healing agent to the top surface (Reproduced from [101] with permission from Elsevier. Copyright 2008).

investigated the effect of network redundancy, template geometry and diameters of the channels, on the Pareto-optimal front generated by this algorithm and implemented the results within self-healing coating experiments [3] to ensure uniform distribution of healing agent with minimum energy cost (figure 17(b)).

It has been shown, through Murray's Law, that the correct choice of internal vascular diameter is crucial in achieving the desired flow rate. These studies have demonstrated that, by determining an optimal solution for microvascular network design through careful consideration of parameters and constraints, it is theoretically possible to design a system that will efficiently deliver the healing agents to a crack site, while minimising the impact on structural integrity. Ultimately, the parameters for optimisation will be highly dependent not only on the material, but also on the network fabrication method, particularly as the latter is likely to place some limit on the overall complexity of the system that can be physically realised, regardless of the optimal solution. Recent developments in AM technologies have now brought about the possibility to design and fabricate vascular networks with geometry based on Murray's Law, due to greater design freedom compared with traditional, subtractive fabrication methods.

4. AM of vascular networks

AM has been defined as '*a process of joining materials to make objects from 3D model data, usually layer upon layer, as opposed to subtractive methodologies*' [102]. Arising in the 1980s with stereolithography, the technology primarily found its way into conceptual and functional prototype production for visualisation purposes and form, fit and function tests, with little regard to structural integrity or mechanical performance of the printed parts [103, 104]. In recent years, extensive technology and material developments, such as improvements in speed, accuracy and material properties, have allowed the potential of this manufacturing process for the

fabrication of tooling, concept parts and end-use parts to be realised, resulting in its adoption across a vast range of industries, from bioengineering to aerospace [105, 106]. Interest has stemmed from the desire to minimise assembly stages, the need to produce more complex parts that incorporate additional functionality, and the ability to create high-end and/or low-volume 'niche' objects [105].

The importance of network design on achieving efficient delivery of fluid to a damage site has already been emphasised and AM shows exciting promise for the fabrication of self-healing networks, due to the ability of these technologies to handle high degrees of geometrical complexity, therefore permitting more efficient VDs, whilst also enabling a reduction in the total number of manufacturing steps required to produce a self-healing material. The number of additive processes is steadily increasing with time, each providing different manufacturing capabilities relating to the available build volume, processing speed, part quality (mechanical performance, dimensional accuracy and surface finish), and the degree of post-processing required to achieve the desired outcome [107]. The more established methods to date include binder jetting (often referred to as 3DP), directed energy deposition (e.g. laser engineered net shaping), material extrusion (e.g. fused deposition modelling, FDM), material jetting (often referred to as inkjet printing), powder bed fusion (e.g. selective laser sintering), sheet lamination (e.g. laminated object manufacturing) and vat polymerisation (e.g. stereolithography), as defined by the ASTM F2921 standard [102]. Detailed reviews of these 3D printing processes can be found in [108–110], in addition to 4D printing technologies (i.e. those which can fabricate parts that are able to their alter shape or properties over time) for smart materials [111, 112].

Numerous 3D direct writing technologies that are capable of printing solely on the microscale also exist. These have primarily been developed for 2D printing purposes but have the capability to fabricate 3D microstructures [113]. For example, DIW (a material jetting process) has been used to create 3D microvascular networks within epoxy-based materials for the transportation of healing agents to cracks sites [3–10, 114]. Hybrid processes, such as shape deposition modelling, utilise both additive and subtractive processes to fabricate 3D parts [113].

Initially, the primary purpose of AM was to produce plastic prototypes and, thus, many of these processes have been developed specifically for polymers. Technological developments have since enabled complex, net-shaped, or nearly net-shaped, functional parts to be made from metals, ceramics and composites [106]. The advances in materials include new formulations of stereolithography resins, new polyamides specifically for laser sintering and the production of a vast range of novel FDM filaments, such as flexible filaments, materials that display conductive and magnetic properties, and those containing carbon and glass reinforcement [105].

AM technologies have been used to create channels for both self-healing and self-cooling applications; however, the most in depth research into 3D printing of vasculature has focused on artificial blood vessels and tissue constructs in medical research [115–117]. Due to the highly complex requirements and varying length scales of these structures; nozzle-, laser- and printer-based methods have all been explored. Here we focus on two particular approaches which we deem most appropriate to the self-healing community: (i) the generation of integrated channels directly within the host matrix, most commonly via sacrificial templating, and (ii) the generation of free-standing tubular structures.

4.1. Sacrificial templating

The simplest approach to introduce a microfluidic network into a structure is to create an interconnected network directly within the host matrix. Initial success in producing such networks has been achieved through soft lithographic techniques [118]. This process, however, is restricted to producing in-plane networks or stacks of in-plane networks, which requires a high number of processing steps. More recently, vasculature has been formed by introducing a sacrificial structure into the matrix, such as in the method used in the VaSC technique discussed earlier in this manuscript [22, 53–55]. Further developments have made use of extrusion-based printing of sacrificial scaffolds which are then casted, and direct-write printing using inks and laser technologies. We discuss these in turn below.

4.1.1. Extrusion-based printing

Moulding printed sacrificial templates into a matrix is an inexpensive and scaleable method for producing vascular networks. Miller *et al* [119] developed a simple casting approach whereby rigid filament networks of carbohydrate glass were 3D printed at temperatures above 100°C and used to construct a sacrificial template of cylindrical networks in a specific geometrical pattern, that was then encapsulated within a polymer matrix. They created sacrificial templates in the form of self-supporting perpendicular lattices, curved filaments and Y-junctions with fibre diameters in the range of 150–750 μm, which could then be dissolved in an aqueous solution (figure 18).

In prior self-healing research, PLA has been adopted as the sacrificial material to produce microvascular channels within a polymer matrix. Initially, commercial PLA fibres were used, which limited the network

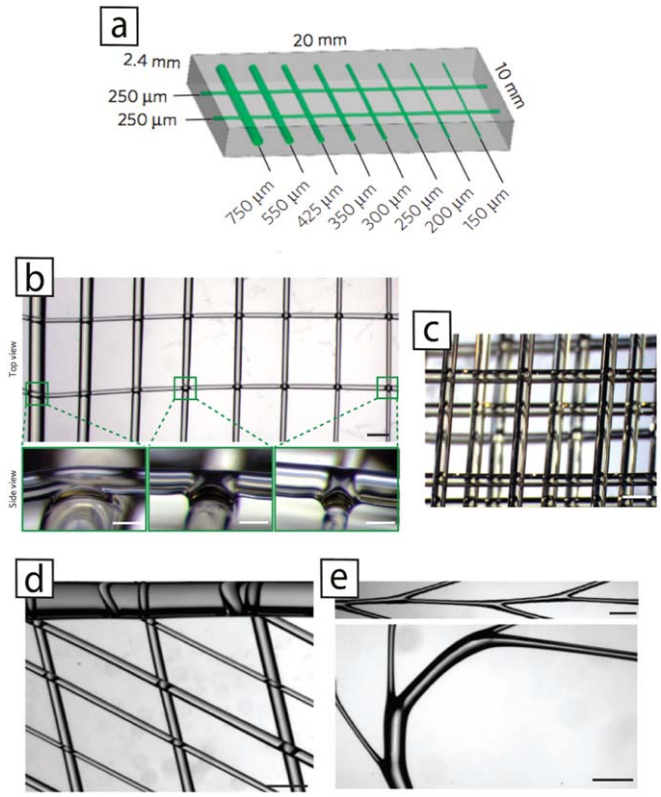

Figure 18. Vascular construction via perfusable channels within 3D hydrogel matrices: (a) design of a multi-scale lattice; (b) top view of (a) printed in carbohydrate glass (scale bar, 1 mm) and a close-up of interfilament fusions (scale bars, 200 μm); (c) multilayered lattices (scale bar, 1 mm); (d) single filament connected to angled arrays of similar filaments (scale bar, 1 mm); (e) serial Y-junctions and curved filaments (scale bars, 1 mm) (Reproduced from [119] with permission from Springer Nature. Copyright 2012).

geometries to one dimension at any one time [22, 53, 54]. Gergely *et al* [55] later produced two-dimensional networks by laser cutting sheets of sacrificial material, followed by 3D PLA architectures using a LulzBot desktop FDM printer; the diameters of the branched structure ranged from 10 mm down to 1.5 mm. The 3D printed structure was painted with a solution of PLA and SnOx catalyst prior to epoxy infusion in order to solidify the walls and aid thermal decomposition. Finally, to vaporise the PLA, the structure was thermally treated at 200 °C for 48 h leaving behind a hollow, branching vascular network within the resin.

Hinton *et al* [120] added a custom syringe-based extruder onto a MakerBot Replicator to print 3D hydrogel structures directly within a secondary hydrogel that acted as a temporary support; a process termed freeform reversible embedding of suspended hydrogels (FRESH). They demonstrated the ability of this process to print arterial bifurcating trees with a wall thickness of less than 1 mm and internal diameters ranging between 1 and 3 mm.

4.1.2. Direct ink writing

In DIW, structures are created by depositing colloid-, nanoparticle-, or organic-based inks layer-by-layer, either through a droplet-based or continuous filament-based approach [121]. Lee *et al* [117] used a 3D direct printing technique to construct sacrificial templates within collagen hydrogel scaffolds using a heated gelatin solution. This solution was printed between the layers of collagen in a layer-by-layer process and then liquefied and drained at 37 °C, leaving a series of hollow channels within the collagen. Li *et al* [122] succeeded in using a combination of mixed gelatin/alginate/chitosan/fibrinogen hydrogels to vertically assemble hollow channels without the need for a supportive sacrificial material.

Advances in the printing of fugitive ink scaffolds have already been alluded to in the discussion on DIW methods for the fabrication of self-healing vasculature. Therriault *et al* [5] used robotic deposition of fugitive organic ink made from a binary mixture of microcrystalline wax and a lower molecular weight organic phase, which was then infiltrated with a photocurable resin and subsequently removed by heating to approximately 75 °C under a soft vacuum. The result was a series of 3D, interconnected microvascular channels approximately 200 μm in diameter. To enable more complex geometries, Wu *et al* [123] used a modified form of the wax-based ink reported previously [4, 5], composed of a mixture of 55% microcrystalline wax (SP19 Strahl and Pitsch) in heavy mineral oil, to create 2D bifurcating microvascular architectures with varying microchannel size and

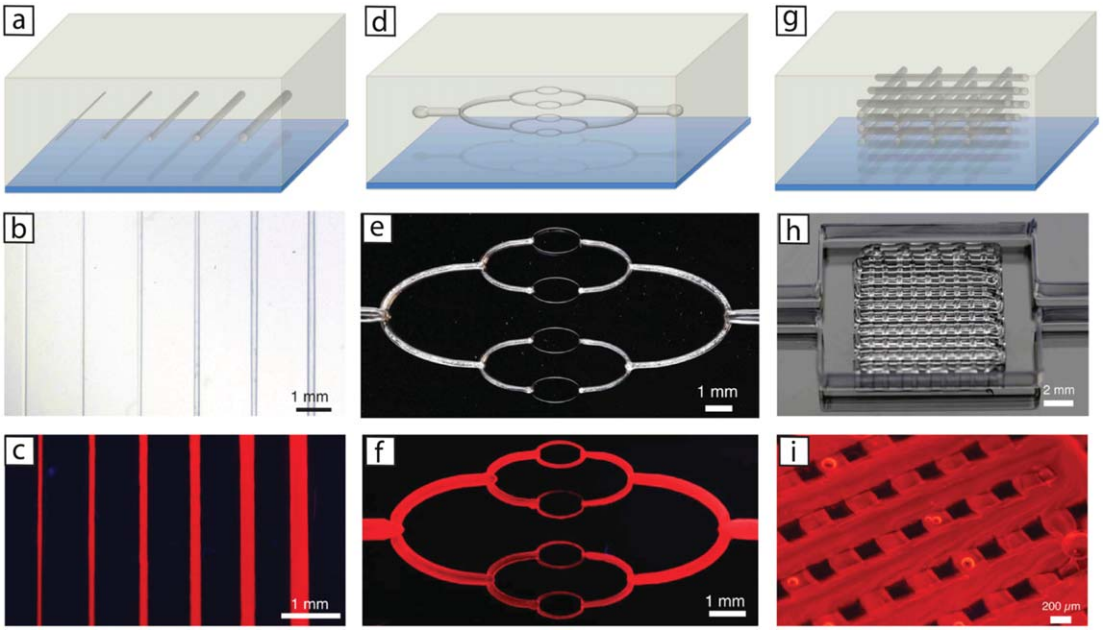

Figure 19. Schematic illustrations, optical images, and fluorescent images of 1D (a)–(c), 2D (d)–(f), and 3D (g)–(i) embedded vascular networks that are printed, evacuated, and perfused with a watersoluble fluorescent dye (Reproduced from [124] with permission from John Wiley and Sons. Copyright 2014).

hierarchical order, within an epoxy matrix. They established that varying the extrusion pressure was the most efficient and reliable method of varying the diameters of the channels while printing.

A series of studies [46, 124] have formed sacrificial networks using an aqueous fugitive ink containing acrylated Pluronic F127®, which exists in liquid form below 4 °C and solidifies when heated, making it easy to print and remove under mild conditions. Using this method, Kolesky *et al* [124] created 2D network designs that were akin to the hierarchical, bifurcating structures found in biological systems, which have evolved to maximise flow of blood and transport of nutrients and waste, while minimising the metabolic cost to the system. Networks with diameters ranging from approximately 650 μm at the inlet/outlet to 150 μm for the smallest branches were printed using a 30 μm nozzle (figure 19).

4.1.3. Direct laser writing

Laser writing creates patterned materials either through ablation, involving the direct removal or deposition of material, selective sintering, which uses a laser to locally fuse a polymer powder, or through reactive chemical processes, such as two-photon polymerisation, laser chemical vapour deposition and stereolithography [121].

Laser-write printing eliminates the problems associated with nozzle clogging, while having the capability to print at high resolution and accuracy with higher viscosity materials. In the studies by Lim *et al* [84] and Kam *et al* [125], direct laser writing was used to micro-machine biomimetic multi-width, multi-depth vasculatures of up to eight generations of bifurcation, on silicon wafers. The channel diameters produced obeyed Murray's law, which, when compared with planar patterning, offered lower overall resistance and more gradual changes in flow velocities due to the varying channel depths. The laser machined silicon structures were then used as a mould to create microvascular channels on polydimethylsiloxane (PDMS). Grigoryan *et al* [126] used photopolymerisable hydrogels, combined with photoabsorbing food additives, to produce transparent hydrogels with intravascular 3D fluid mixers and functional bicuspid valves, and a series of entangled vascular networks, aimed at promoting fluid flow.

More recently, Huang *et al* [127] used electron beam irradiation, rather than a laser, to locally vaporise and fracture plastic material through electrostatic discharge, enabling highly-branched, tree-like 3D microvascular networks with varying channel diameters to form instantaneously within the substrate material. They tested this fabrication process in both PMMA and PLA and successfully achieved vascular diameters ranging from 500 μm at the trunk of the tree to 10 μm near the tip for PMMA, and 300 μm and 20 μm respectively for PLA, demonstrating the potential of this method for rapid, multi-scale vascular fabrication that could scale up to mass production.

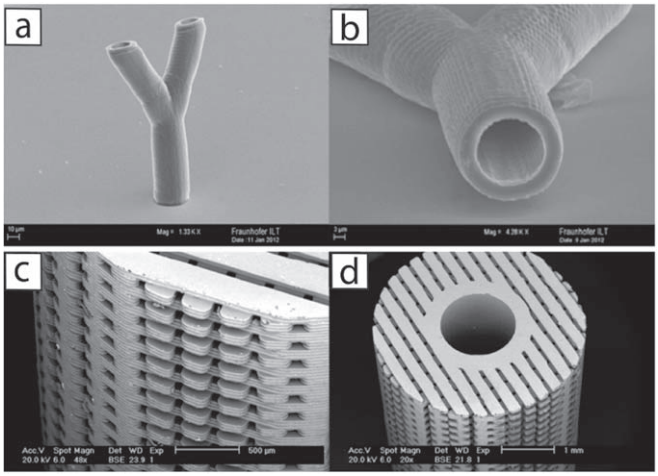

Figure 20. Free standing vasculature: SEM images of (a), (b) a branched structure generated via two-photon polymerisation (Reproduced from [116] under CC BY-NC-SA 3.0); (c), (d) a porous vascule fabricated from a photopolymer via microstereolithography ([130], reproduced from [131] with permission from IOP Publishing, Ltd.).

4.2. Free-standing tubular structures

An alternative approach to creating artificial networks is through the manufacture of freestanding tubular structures. The fundamental challenge in direct printing of freestanding vasculature is the tendency of channels to sag or collapse under their own weight. Addressing this requires careful selection of material, processing parameters and in some cases, support material that can be removed after printing. We discuss some of the recent advances below, which, although focus primarily on tissue engineering, have the potential to act as inspiration for the development of vasculature in engineering-based, performance materials.

4.2.1. Stereolithography

Preference in the creation of free-standing vascules has been given to the use of a photo-curable resin in stereolithographic techniques as this eliminates many problems associated with structural support and enables high-resolution features to be introduced. Engelhardt *et al* [128] and Meyer *et al* [116] fabricated branched vascular networks from photo-cross-linkable synthetic polymers and biopolymers using a combination of stereolithography and two-photon polymerisation, achieving structures in the 10–100 μm range (figures 20(a) and (b)). Arcuate *et al* [129] used stereolithography to create branched networks in bulk poly(ethylene glycol)-dimethacrylate (PEG-dma) gel, with varying internal channel orientations and structures with more than one material in a single layer.

Photo-elastomers have also been used to create vascules via microstereolithography. Research conducted by Schuster *et al* [130] led to vascules that had some 3D microstructure architecture contained within the vascule walls, resulting in a high degree of porosity within the structures (figures 20(c) and (d)). Baudis *et al* [131] furthered this by exploring possible resin combinations in order to improve structural properties.

4.2.2. Inkjet printing

Inkjet printing has successfully been used to fabricate hydrogel-based vascular structures through the use of calcium chloride ($CaCl_2$)-based alginate solutions [132–134]. This technique has the advantage of being able to process multiple materials during assembly, which is not possible in photopolymerisation methods. Research conducted by Kesari *et al* [135] found that the dimensions of the vascular constructs were ultimately limited due to the difficulty in printing layer-by-layer high-aspect ratio structures. Nakamura *et al* [136–138] showed that, by varying the diameter of the microgel beads, it is possible to obtain some degree of control over the wall thickness and inner diameter of the vascules. This successfully resulted in the printing of linear tubes that were several centimetres long, with wall thicknesses between 35 and 40 μm and a bore size in the range of 30–200 μm.

Further advances in inkjet printing of alginate droplets in $CaCl_2$ solution have shown that, through careful selection of processing parameters, it is possible to print 3D tubular structures with heights of up to 10 mm and overhangs of up to 63°. Yet the specific deposition of ink droplets for vascular fabrication remains highly complex due to the tightly controlled conditions required to support the structures during the build process, which limits the overall resolution of the outputs [115, 139]. Scientists at the Fraunhofer Institute have combined inkjet printing and stereolithography to produced finely detailed, branched, porous blood vessels from an acrylate-based synthetic polymer, with layer thicknesses of approximately 20μm and pore sizes in the

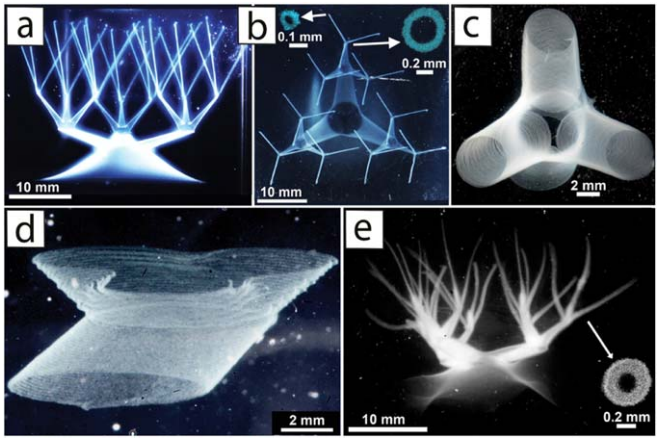

Figure 21. Hierarchically branched tubular structures: (a), (b) a continuous, highly-branched network of hollow vessels printed in a granular medium (insets: confocal cross-sections); (c), (d) high-resolution photos of one of the junctions of the branched network showing the hollow tubes with thin walls and features approximately 100 μm in diameter with complex curvatures; (e) a crosslinked network after removal from the granular gel, photographed in water (inset: confocal cross-section) (Reproduced from [142] with permission from the authors. Copyright 2015).

hundreds of microns [140]. Although inkjet printers are relatively inexpensive and typically fast at printing, shortcomings include nozzle clogging, cavitation bubbles and selective ink viscosity when fabricating vascular networks [141].

4.2.3. Extrusion-based printing

Extrusion of hierarchically branching networks has been achieved by the direct writing of PDMS and photoreactive PVA into a supporting slurry of Carbopol hydrogel microparticles, removing limitations placed by surface tension, gravity and particle diffusion (figure 21). As the nozzle of the extruder moves freely within the slurry, the gel becomes fluid at the point of injection and then quickly solidifies, locking the deposited material in place. Once the PVA has crosslinked after printing, the structure is removed from the slurry by immersing in a gently agitated water bath [142].

Several studies have made use of coaxial nozzles to extrude hollow fibres from Ca-alginate systems [143, 144]. Luo *et al* [145] created hollow alginate fibres ranging between 200μm to the millimetre-scale, using a concentrated alginate/PVA paste and shell/core nozzles. The shell/core nozzle tip was formed by placing a right angle stainless steel nozzle with a smaller diameter (core nozzle) into a conic plastic nozzle with a larger diameter (shell nozzle). The diameters of the hollow fibres could be varied by changing the diameter of the shell-core nozzles.

Jia *et al* [146] also used a multilayered coaxial extrusion system (figures 22(a) and (b)) to continuously extrude single hollow tubes of different shapes and architectures, both single-layer and stacked (figures 22(c)–(h)). The coaxial nozzle device contained two injection channels with varying sizes of external and internal needles, and was used to deposit a blend bioink based on GelMA, sodium alginate, and 4-arm poly(ethylene glycol)-tetra-acrylate (PEGTA). They showed that by switching on/off the bioink flow in the outmost channel of the printhead, or by changing the flow rates of the bioink extrusion and/or moving speed of the printhead, they could vary the diameter of a single tube without changing needle sizes (figures 22(i)–(j)). Zhang *et al* [143, 144] also confirmed that the diameters could be increased by increasing the alginate dispensing rate, and the core-to-filament ratio diameter could be altered by changing the relative speed between the $CaCl_2$ flow and alginate flow; the latter was possibly due to a combination of increased diffusion rate through the alginate network and higher radial forces placed on the wall of the filament.

At a larger length scale, free-standing vasculature has also been fabricated from thermoplastic polycaprolactone (PCL) via nozzle-based extrusion, using polyvinyl alcohol (PVA) as a support material that can be removed with water. Visser *et al* [147] produced stiff, multi-branched vascular networks from PCL using PVA as a support with dimensions of $67 \times 42 \times 8\ mm^3$ ($L \times W \times H$) and a bore decreasing from 4 to 2 mm. They also produced vascular tubes with diameters of approximately 5 mm and wall thicknesses between 2 and 5 mm, from a gelatin-methacryloyl hydrogel (GelMA) using Ca-alginate as the support. Skardal *et al* [148–150] used the Fab@Home nozzle-based extrusion printer to fabricate tubular structures using materials such as photo-cross-linkable gelatin along with photo-cross-linkable hyaluronic acid (HA), and thiol-modified gelatin with thiol-modified HA.

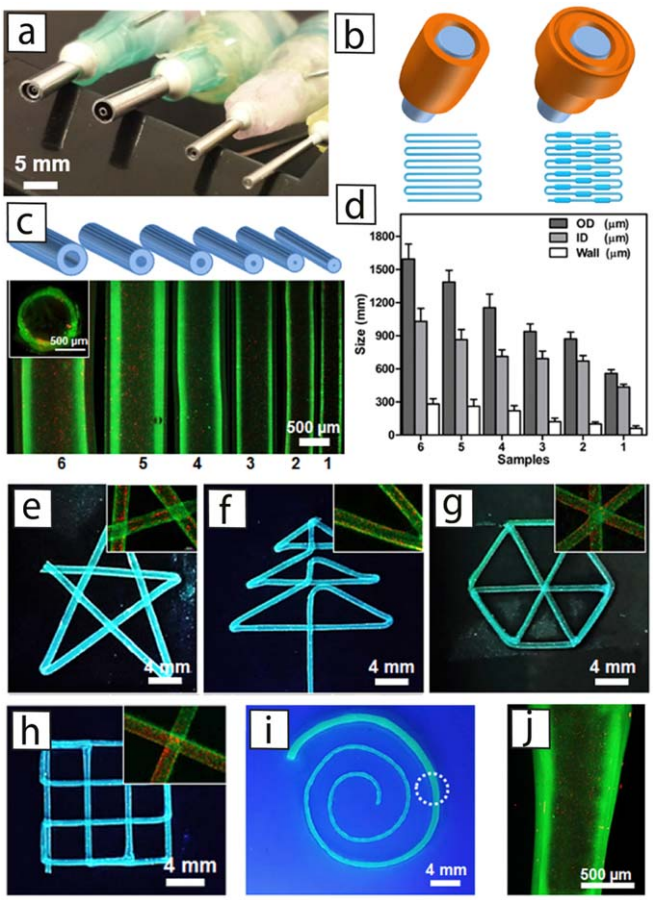

Figure 22. (a) Multilayered coaxial nozzles and (b) schematic showing the fabrication of free-standing hollow tubes with constant diameter (left) and changeable sizes (right); (c) schematic and representative fluorescence micrographs showing printed tubes with varying outer diameters and (d) data showing achieved vascule dimensions; (e)–(h) fluorescence photographs showing printed tubes with various shapes, where green fluorescent beads were embedded into the walls during printing; the insets are high-magnification images; (i) photograph showing a single tube printed with a gradually increasing size; magnified in (j) (Reproduced from [146] with permission from Elsevier. Copyright 2016).

4.3. Challenges in 3D printing vasculature

This perspective article has introduced the current state of the art for subtractive and additive healing constructs through traditional and novel sacrificial chemistry. It has also introduced the design methodologies considered in the creation of a vascular network and how these architectures can be realised by additive fabrication methods. In the following subsections, we identify a number of key areas which will require further refinement to realise the full potential of creating integrated channels (using sacrificial templating) and the generation of free-standing tubular structures by AM.

4.3.1. Structural integration

Fundamentally, a self-healing multifunctional material must satisfy its primary functions; to achieve these dual-goals the healing entity must succinctly integrate within the host architecture without compromising performance. In bulk polymers, or as a surface coating, this is readily achievable but in advanced composites, the challenge is more complicated as the healing network is in direct 'competition' with the volume occupied by the structural fibres. When the introduction of a new functionality introduces additional design constraints that compromise the original intent, there is a need for new digital tools to design and optimise the performance of the system *a priori*. These new approaches for AM, whether new algorithms or models for bi-material optimisation linked to multiscale structural simulations, which capture realistic manufacturing approaches, are essential to design and optimise 'structural' vascular systems required today and in the foreseeable future.

4.3.2. Network junctions

Creating 3D networks is a difficult task in the manufacture of vascular networks. The junction points are critical as they will influence the flow characteristics of the healing medium and act as potential blockage points, particularly for small vessel sizes, and thus have a significant influence on the self-healing efficiency of the system

[44]. To manufacture a 3D network in a single processing step with existing 3D printing methods will require the construction, and subsequent removal, of additional scaffolds to support large overhangs. This significantly complicates the manufacturing process. An alternative method to fabricate 3D networks could make use of connectors at each junction point to connect individual 1D and 2D network elements; however, these must be designed to have minimum interference on the flow, which itself can be challenging as the branching flow effects in these regions are complex and difficult to model [151].

4.3.3. Material properties

Depending on the AM process employed, the strength of parts built by AM processes are highly directional in comparison to those made by conventional processes and is linked to the build orientation. This anisotropy can lead to points of significant weakness in the structure [152]. New materials with improved properties, for example less brittle, lower shrinkage and better processing, are continually being commercialised [153]. These materials are typically thermoplastics, metals or ceramics. Thermosetting materials, such as those which are found within the composites industry, have not yet been suitably adapted for AM processes [154].

4.3.4. Size limitations

Producing large networks using some AM technologies remains challenging due to a lack of material strength, and is often impractical due to the time and cost required to complete the build process; a consequence of relatively slow machine throughput and expensive equipment and materials [106, 155]. In addition, many 3D printers have an enclosed build volume which may limit the network size that can be printed [154]. New hardware ideas and concepts for the base plate and printing carousel are required to permit 3D printing of large structures with high local resolution. Movement towards delta-robot printing is one viable approach to achieve this.

4.3.5. Software limitations

AM processes are capable of producing complex shapes with varying material properties and even structures that can exhibit some degree of multifunctionality. However, most 3D computer-aided design software has been developed with subtractive processes in mind, limiting the technology from reaching its full potential. Future software needs to have the ability to represent complex geometries, including sub-structures and multiple materials, whilst also being able to consider processing parameters, how these may affect the final part and how they may be optimised. This highlights the need to develop process-structure-property relationships [106]. In addition, the errors that occur during facet approximation in the formation of STL files must be eliminated and the adoption of new file formats is currently underway [103, 153, 156, 157]. Design for AM (also known as DfAM), which is necessary to ensure optimal manufacture of parts and reduced costs by integrating manufacturability directly into the design phase, remains a key challenge for engineers. This limitation is largely due to the need to embody material distribution, complex hierarchical structures, model and topology optimisation with CAD tools and incorporate specific AM capabilities and constraints into the part design, which also vary with the type of AM process. This requires a complete rethink into current design processes in order to avoid fixing on designs in early conceptual stages.

4.3.6. Part accuracy

There are several factors that can affect how accurately the output matches the 3D computer model, which, in turn, may also affect both the repeatability and consistency of manufacture. In addition, current AM systems have restricted ability to monitor and control the build process and respond to *in situ* feedback. One such factor is the available printing resolution which is influenced by aspects such as nozzle size for material extrusion, X and Y printer resolution and Z step height. This imposes limitations on layer thickness and minimum wall heights [154]. Due to the layerwise process, fabricated parts tend to have a rough or ribbed surface finish which could inhibit the flow of healing agents [155]. Depending on the method of fabrication, post-processing of parts to improve the surface finish is possible and differing degrees of success have been reported using techniques such as ultraviolet (UV) treatment, sanding, heat treatment and acetone vapour treatment [158, 159]. The greatest sources of inaccuracy are due to material shrinkage and distortion, particularly with extrusion processes, which occur as the material is cooled down. This may lead to stresses within the part which eventually creep and cause the material to warp. The likelihood of these distortions can be minimised either by selecting a material with small shrinkage or through careful control of the printing process, such as minimising the heat differential between the nozzle and external atmosphere [106, 153].

5. Conclusion and future directions

Self-healing materials have been proposed as an alternative solution to the repair of damage in fibre-reinforced structures, sandwich panels and bulk polymer materials. Many of the latest developments have focused on vascularised structures due to their ability to transport healing agents over a large distance from an external reservoir; however, limitations still exist in the number of healing cycles that can be achieved and the location of damage, which must be in close proximity to the network. Recent advances in AM have opened up the design space and could enable healing to be achieved more efficiently over a greater damage volume.

Network design plays a crucial role in ensuring the healing agents fill the damage site as quickly and efficiently as possible without prior knowledge of its location. Various relationships between parent and daughter vascules have been proposed in order to minimise the global resistance of the network to flow whilst considering minimal disruption to the host material. Due to a lack of developments in manufacturing methods, few of these designs have been implemented; however, AM permits more complex network designs that can lead to improved coverage of the material volume.

AM has been used to fabricate vascular networks for tissue-based applications, predominantly through nozzle extrusion, stereolithography and inkjet printing, yet, to date, there is little exploration into self-healing applications. Furthermore, although AM has numerous advantages, including the ability to fabricate complex geometries, an importance must now be placed on gaining a better understanding of how the manufacturing method, material properties and software influence the overall design process. Nevertheless, AM processes remain an exciting collection of technologies for the manufacture of vascular networks, opening up design freedoms and bringing about the ability to take a new approach to vascularised self-healing which has not previously been achieved.

Given all these advances in network design and AM, what does the future hold for the field of multifunctional vascular self-healing? In the authors' opinion, the most important topics and research directions can be grouped under three main thematic areas (namely 'VD', 'HC' and 'AM') which can be further subdivided into eight grand challenges that are likely to have major breakthroughs, significant research, and/or socioeconomic impact in the next 10–15 years.

Figure 23 captures the Grand Challenges and their interaction across the three thematic areas for enabling repair autonomy through the generation of self-healing vascular networks. As the figure illustrates, a number of common challenges reside across the different thematic areas. For example, 'remodelling HC' while residing directly within the 'HC' thematic area, also has a direct bearing and profound impact upon 'VD'. Equally, 'resilient network design' can be found under both 'AM' and 'VD' due to the need to consider the interplay of both aspects when deriving the final solution. Similarly, the need to employ 'simulation'; is also common across all three thematic areas; whether this is the modelling of resin cure kinetics and resultant properties, to predict the fluid flow in the network or to ascertain the structural performance/continuity of the network and structure before and after the healing event. Of these three areas, engineering design tools already exist to simulate fluid flow and structural continuity, however, new simulation tools are required to predict the healing response of the system which is why it is included as a Grand Challenge.

In an effort to assist the reader, the eight Grand Challenges are grouped and designated according to the influence they exert on the three different thematic areas (VD, HC and AM). In general, each challenge is associated with one area but in some cases two or three thematic areas are designated.

(i) *Functionally graded networks* (*AM*) would utilise a self-healing 'vascular network' whose variation in size, location and 'volume fraction' would be dependent upon local-global design requirements. The self-healing functionality would transition throughout the structure and be optimised against the nature and magnitude of the threat.

(ii) *Resilient network design* (*AM; VD*) by creating a vascular network which delivers healing potential without fracturing, or has built in redundancy, thus maintaining its structural and flow continuity throughout the damage event-healing cycle.

(iii) *Healing under load*; (*HC*) the ability to heal under a static or cyclic load (which has caused the original fracture/failure) is the ultimate challenge for the self-healing community. To date, this has been under limited conditions in vascular structures and a new philosophy is required which allows a healing material to bridge the fracture plane and gradually increase its structural performance to inhibit any further damage growth and then ultimately attain full structural performance.

(iv) *Adaptive healing* (*HC*) systems proactively change the healing behaviour of the resin according to the demands of the internal stress state and the operating environment rather than employing two-part chemistry with a fixed stress-strain profile. It is envisaged that the 'adaptive system' will intuitively collect

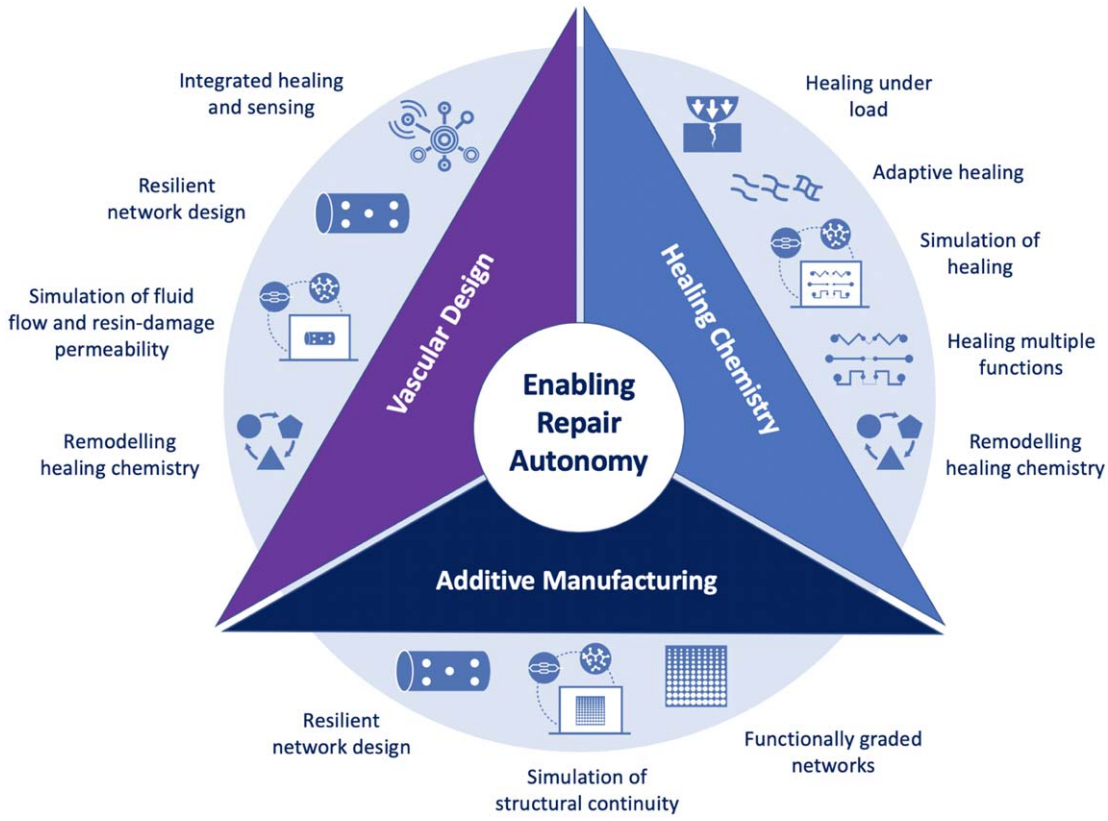

Figure 23. Grand challenges in the design and manufacture of self-healing vascular networks.

information about its internal state and subsequently change the HC depending upon the system's need. The adaptive healing system will be proactive and adapt the healing resin's stiffness and strain-to-failure response depending upon the magnitude of the threat.

(v) *Simulation of healing* (*AM; HC; VD*) which would capture flow within the network, flow into damage, the changing cure kinetics, the change in mechanical performance of the resin locally and the restoration of the local/global structural performance when subjected to loading.

(vi) *Healing of multiple functions* (*HC*) simultaneously; due to component complexity, the next generation of self-healing materials will have to impart the restoration of both primary and secondary structural functionality simultaneously, e.g. toughness and transparency would be required for glass screens; high conductivity and structural repairs will be needed for self-healing batteries, solar cells, flexible electronics and energy storage devices.

(vii) *Integrated self-healing and sensing* (*VD*) within the network would provide the designer/operator with direct feedback on the state of the structure's performance before, during and after self-healing. The operational capability of the 'vessel' after it has been healed can then be ascertained and its operational role optimised according to this data.

(viii) *Remodelling HC* (*VD*) where at the onset of damage, the material autonomously alters the local stress state (by allowing compliance to give compartmentalisation) to ensure global structural fracture is avoided, before returning subsequently to full load carrying capability. This is analogous to a 'shape memory' attribute found in smart materials but directed towards a 'remodelling memory' for stress or strain.

In conclusion, it should be noted that the field of vascular self-healing covers many underpinning and associated scientific areas, i.e. chemistry, design, engineering, materials science and physics. The identification of the challenges above is neither exclusive nor exhaustive and there are likely to be many topics not listed that are equally important for future development. However, it is imperative that multidisciplinary or transdisciplinary teams across these disciplines are developed to tackle these challenges if commercial products are to exhibit 'mammalian or plantae' sensing, healing and remodelling on demand.

Acknowledgments

This work was supported by the Engineering and Physical Sciences Research Council through the EPSRC Centre for Doctoral Training in Advanced Composites for Innovation and Science [grant number EP/G036772/1], the University of Bristol 2016-2017 EPSRC Doctoral Training Partnership [grant number EP/N509619/1] and the EPSRC Engineering Fellowship for Growth [grant number EP/M002489/1].

ORCID iDs

Isabel P S Qamar https://orcid.org/0000-0002-1311-4301
Nancy R Sottos https://orcid.org/0000-0002-5818-520X
Richard S Trask https://orcid.org/0000-0002-8082-8179

References

[1] Plaisted T A and Nemat-Nasser S 2007 *Acta Mater.* **55** 5684–96
[2] Rule J D, Sottos N R and White S R 2007 *Polymer* **48** 3520–9
[3] Toohey K S, Sottos N R, Lewis J A, Moore J S and White S R 2007 *Nat. Mater.* **6** 581–5
[4] Therriault D, White S R and Lewis J A 2003 *Nature* **2** 265–71
[5] Therriault D, Shepherd R F, White S R and Lewis J A 2005 *Adv. Mater.* **17** 395–9
[6] Toohey K S, Hansen C J, Lewis J A, White S R and Sottos N R 2009 *Adv. Funct. Mater.* **19** 1399–405
[7] Hansen C J, Wu W, Toohey K S, Sottos N R, White S R and Lewis J A 2009 *Adv. Mater.* **21** 4143–47
[8] Hansen C J, White S R, Sottos N R and Lewis J A 2011 *Adv. Funct. Mater.* **21** 4320–6
[9] Hamilton A R, Sottos N R and White S R 2010 *Adv. Mater.* **22** 5159–63
[10] Hamilton A R, Sottos N R and White S R 2012 *J. R. Soc. Interface* **9** 1020–8
[11] Hayes S A, Zhang W, Branthwaite M and Jones F R 2007 *J. R. Soc. Interface* **4** 381–7
[12] Brown E N, Sottos N R and White S R 2002 *Exp. Mech.* **42** 372–9
[13] Brown E N, White S R and Sottos N R 2004 *J. Mater. Sci.* **39** 1703–10
[14] Brown E N, White S R and Sottos N R 2005 *Comput. Sci. Technol.* **65** 2466–73
[15] Kessler M R and White S R 2001 *Composites* A **32** 683–99
[16] Kessler M R, Sottos N R and White S R 2003 *Composites* A **34** 743–53
[17] Trask R S and Bond I P 2006 *Smart Mater. Struct.* **15** 704–10
[18] Trask R S, Williams G J and Bond I P 2007 *J. R. Soc. Interface* **4** 363–71
[19] Norris C J, Bond I P and Trask R S 2011 *Composites* A **42** 639–48
[20] Norris C J, Bond I P and Trask R S 2011 *Comput. Sci. Technol.* **71** 847–53
[21] Norris C J, Meadway G J, O'Sullivan M J, Bond I P and Trask R S 2012 *Smart Mater. Struct.* **21** 094027
[22] Patrick J F, Hart K R, Krull B P, Diesendruck C E, Moore J S, White S R and Sottos N R 2014 *Adv. Mater.* **26** 4302–8
[23] Williams H R, Trask R S and Bond I P 2007 *Smart Mater. Struct.* **16** 1198–207
[24] Williams H R, Trask R S and Bond I P 2008 *Comput. Sci. Technol.* **68** 3171–7
[25] Qamar I 2017 Development of 3D printed vascular networks for repeated self-healing *PhD Thesis* University of Bristol
[26] Mattsson J, Sung Z and Berleth T 1999 *Development* **126** 2979–91
[27] Berleth T, Mattsson J and Hardtke C S 2000 *Trends Plant Sci.* **5** 387–93
[28] Ritman E L 2005 *Proc. Am. Thoracic Soc.* **2** 477–80
[29] Nowogrodzki A 2018 *Nature* **563** 24–6
[30] Blaiszik B J, Kramer S L B, Olugebefola S C, Moore J S, Sottos N R and White S R 2010 *Annu. Rev. Mater. Res.* **40** 179–211
[31] Garcia S J 2014 *Eur. Polym. J.* **53** 118–25
[32] Post W, Cohades A, Michaud V, van der Zwaag S and Garcia S 2017 *Compos. Sci. Technol.* **152** 85–93
[33] White S R, Sottos N R, Geubelle P H, Moore J S, Kessler M R, Sriram S R, Brown E N and Viswanathan S 2001 *Nature* **409** 794–7
[34] Rule J D, Brown E N, Sottos N R, White S R and Moore J S 2005 *Adv. Mater.* **17** 205–8
[35] Yuan Y, Rong M Z, Zhang M Q, Chen J, Yang G and Li X 2008 *Macromolecules* **41** 5197–202
[36] Yin T, Rong M Z, Zhang M Q and Yang G C 2007 *Comput. Sci. Technol.* **67** 201–12
[37] Yin T, Rhong M Z, Wu J, Chen H and Zhang M Q 2008 *Composites* A **39** 1479–87
[38] Patel A J, Sottos N R, Wetzel E D and White S R 2010 *Composites* A **41** 360–8
[39] Coope T S, Mayer U F J, Wass D F, Trask R S and Bond I P 2011 *Adv. Funct. Mater.* **21** 4624–31
[40] Moll J L, Jin H, Mangun C L, White S R and Sottos N R 2013 *Compos. Sci. Technol.* **79** 15–20
[41] Kim S Y, Sottos N R and White S R 2019 *Compos. Sci. Technol.* **175** 122–7
[42] Norris C J, White J A P, McCombe G, Chatterjee P, Bond I P and Trask R S 2011 *Adv. Funct. Mater.* **21** 3624–33
[43] Williams H R, Trask R S and Bond I P 2011 *Proc. Inst. Mech. Eng.* O **225** 435–49
[44] Williams H R, Trask R S, Knights A C, Williams E R and Bond I P 2008 *J. R. Soc. Interface* **5** 735–47
[45] Patrick J F, Sottos N R and White S R 2012 *Polymer* **53** 4231–40
[46] Wu W, DeConinck A and Lewis J A 2011 *Adv. Mater.* **23** H178–83
[47] Plaisted T A, Amirkhizi A V and Nemat-Nasser S 2006 *Int. J. Fract.* **141** 447–57
[48] Kousourakis A, Mouritz A P and Bannister M K 2006 *Compos. Struct.* **75** 610–8
[49] Kousourakis A, Bannister M K and Mouritz A P 2008 *Composites* A **39** 1394–403
[50] Trask R S and Bond I P 2010 *J. R. Soc. Interface* **7** 921–31
[51] Huang C Y, Trask R S and Bond I P 2010 *J. R. Soc. Interface* **7** 1229–41
[52] Luterbacher R, Trask R S and Bond I P 2016 *Smart Mater. Struct.* **25** 015003
[53] Esser-Khan A P, Thakre P R, Dong H, Patrick J F, Vlasko-Vlasov V K, Sottos N R, Moore J S and White S R 2011 *Adv. Mater.* **23** 3654–8
[54] Dong H, Esser-Kahn A P, Thakre P R, Patrick J F, Sottos N R, White S R and Moore J S 2012 *ACS Appl. Mater. Interfaces* **4** 503–9

[55] Gergely R C R, Pety S J, Krull B P, Patrick J F, Doan T Q, Coppola A M, Thakre P R, Sottos N R, Moore J S and White S R 2015 *Adv. Funct. Mater.* **25** 1043–52
[56] Murray C D 1926 *J. Gen. Physiol.* **12** 207–14
[57] Sutera S P and Skalak R 1993 *Annu. Rev. Fluid Mech.* **25** 1–19
[58] Murray C D 1926 *J. Gen. Physiol.* **9** 835–41
[59] Roux W 1878 *Jena Z. Naturwiss.* **12** 205
[60] Hess W R 1913 Das Prinzip des kleinsten Kraftverbrauches im Dienste hämodynamischer Forschung *Archiv f. Physiol.* **1914** 1–62
[61] Uylings H B M 1977 *Bull. Math. Biol.* **39** 509–20
[62] Roy A G and Woldenberg M J 1982 *Bull. Math. Biol.* **44** 349–60
[63] Sherman T F 1981 *J. Gen. Physiol.* **78** 431–53
[64] Sherman T F, Popel A S, Koller A and Johnson P C 1989 *J. Theor. Biol.* **136** 245–65
[65] Woldenberg M J and Horsfield K 1983 *J. Theor. Biol.* **104** 301–18
[66] Zamir M, Medeiros J A and Cunningham T K 1979 *J. Gen. Physiol.* **74** 537–48
[67] Zamir M and Brown N 1983 *J. Biomech.* **16** 857–63
[68] Zamir M and Brown N 1982 *Am. J. Anat.* **163** 295–307
[69] Zamir M and Medeiros J A 1982 *J. Gen. Physiol.* **79** 353–60
[70] Zamir M 1982 *Bull. Math. Biol.* **44** 597–607
[71] Zamir M, Sinclair P and Wonnacott T H 1992 *J. Biomech.* **25** 1303–10
[72] Taber L A, Ng S, Quesnel A M, Whatman J and Carmen C J 2001 *J. Biomech.* **34** 121–4
[73] Price C A, Knox S J C and Brodribb T J 2013 *PLoS One* **8** e85420
[74] Horn H S 2000 Twigs, trees, and the dynamics of carbon in the landscape *Scaling in Biology* (Oxford: Oxford University Press) pp 199–220
[75] West G B, Brown J H and Enquist B J 1997 *Science* **276** 122–6
[76] West G B, Brown J H and Enquist B J 1999 *Nature* **400** 664–7
[77] McCulloh K A, Sperry J S and Adler F R 2003 *Nature* **421** 939–42
[78] McCulloh K A, Sperry J S and Adler F R 2004 *Funct. Ecol.* **18** 931–8
[79] McCulloh K A and Sperry J S 2005 *Am. J. Bot.* **92** 985–9
[80] Cabodi M, Choi N W, Gleghorn J P, Lee C S, Bonassar L J and Stroock A D 2005 *J. Am. Chem. Soc.* **127** 13788–9
[81] Ling Y, Rubin J, Deng Y, Huang C, Demirci U, Karp J M and Khademhosseini A 2007 *Lab Chip* **7** 756–62
[82] Golden A P and Tien J 2007 *Lab Chip* **7** 720–5
[83] Bellan L M, Pearsall M, Cropek D M and Langer R 2012 *Adv. Mater.* **24** 5187–91
[84] Lam D, Kamotani Y, Cho B, Mazumder J and Takayama S 2003 *Lab Chip* **3** 318–23
[85] Emerson D R, Cieslicki K, Gu X and Barber R W 2006 *Lab Chip* **6** 447–54
[86] Barber R W and Emerson D R 2008 *Microfluid. Nanofluid.* **4** 179–91
[87] Barber R W and Emerson D R 2010 *ATLA* **1** 67–79
[88] Bejan A and Lorente S 2006 *J. Appl. Phys.* **100** 041301
[89] Bejan A 2000 *Shape and Structure, from Engineering to Nature* (Cambridge: Cambridge University Press)
[90] Bejan A, Rocha L A O and Lorente S 2000 *Int. J. Therm. Sci.* **39** 949–60
[91] Bejan A and Lorente S 2013 *J. Appl. Phys.* **113** 151301
[92] Bejan A, Lorente S and Wang K M 2006 *J. Appl. Phys.* **100** 033528 (https://aip.scitation.org/doi/abs/10.1063/1.2218768?journalCode=jap)
[93] Wang K M, Lorente S and Bejan A 2006 *J. Phys. D: Appl. Phys.* **39** 3086–96
[94] Wang K M, Lorente S and Bejan A 2007 *J. Phys. D: Appl. Phys.* **40** 4740–9
[95] Hall J, Qamar I P S, Rendall T C S and Trask R S 2015 *Smart Mater. Struct.* **24** 037002
[96] Williams H R, Trask R S, Weaver P M and Bond I P 2008 *J. R. Soc. Interface* **5** 55–65
[97] Kim S, Lorente S and Bejan A 2006 *J. Appl. Phys.* **100** 063525
[98] Lee J, Kim S, Lorente S and Bejan A 2008 *Int. J. Heat Mass Transfer* **51** 2029–40
[99] Cetkin E, Lorente S and Bejan A 2010 *J. Appl. Phys.* **107** 114901
[100] Lorente S and Bejan A 2009 *J. Porous Media* **12** 1–18
[101] Aragon A M, Wayer J K, Geubelle P H, Goldberg D E and White S R 2008 *Comput. Methods Appl. Mech. Eng.* **197** 4399–410
[102] ASTM Standard F2792-12a 2012 *Standard Terminology for Additive Manufacturing Technologies* (PA: West Conshohocken)
[103] Kai C C 1994 *Comput. Control Eng. J.* **5** 200–6
[104] Mellor S, Hao L and Zhang D 2014 *Int. J. Prod. Econ.* **149** 194–201
[105] Campbell I, Bourell D and Gibson I 2012 *Rapid Prototyp. J.* **18** 255–8
[106] Guo N and Leu M C 2013 *Front. Mech. Eng.* **8** 215–43
[107] Conner B P, Manogharan G P, Martof A N, Rodomsky L M, Rodomsky C M, Jordan D C and Limperos J W 2014 *Addit. Manuf.* **1–4** 64–76
[108] Gibson I, Rosen D and Stucker B 2015 *Development of Additive Manufacturing Technology* (New York, NY: Springer New York)
[109] Ngo T D, Kashani A, Imbalzano G, Nguyen K T and Hui D 2018 *Composites* B **143** 172–96
[110] Wang X, Jiang M, Zhou Z, Gou J and Hui D 2017 *Composites* B **110** 442–58
[111] Khoo Z X, Teoh J E M, Liu Y, Chua C K, Yang S, An J, Leong K F and Yeong W Y 2015 *Virtual Phys. Prototyp.* **10** 103–22
[112] Wu J, Zhao Z, Kuang X, Hamel C M, Fang D and Qi H J 2018 *Multifunct. Mater.* **1** 015002
[113] Vaezi M, Seitz H and Yang S 2013 *Int. J. Adv. Manuf. Technol.* **67** 1721–54
[114] Olugebefola S C, Aragón A M, Hansen C J, Hamilton A R, Kozola B D, Wu W, Geubelle P H, Lewis J A, Sottos N R and White S R 2010 *J. Compos. Mater.* **44** 2587–603
[115] Hoch E, Tovar G E M and Borchers K 2014 *Eur. J. Cardio-Thorac.* **46** 767–78
[116] Meyer W, Engelhardt S, Novosel E, Elling B, Wegener M and Krüger H 2012 *J. Funct. Biomater.* **3** 257–68
[117] Lee W, Lee V, Polio S, Keegan P, Lee J H, Fischer K, Park J K and Yoo S S 2010 *Biotechnol. Bioeng.* **105** 1178–86
[118] McDonald J C, Duffy D C, Anderson J R, Chiu D T, Wu H, Schueller O J A and Whitesides G M 2000 *Electrophoresis* **21** 27–40
[119] Miller J S *et al* 2012 *Nat. Mater.* **11** 768–74
[120] Hinton T J, Jallerat Q, Palchesko R N, Park J H, Grodzicki M S, Shue H J, Ramadan M H, Hudson A R and Feinberg A W 2015 *Sci. Adv.* **1** e1500758
[121] Lewis J A and Gratson G M 2004 *Mater. Today* **7** 32–9

[122] Li S, Xiong Z, Wang X, Yan Y, Liu H and Zhang J 2009 *J. Bioact. Compat. Polym.* **24** 249–65
[123] Wu W, Hansen C J, Aragón A M, Geubelle P H, White S R and Lewis J A 2010 *Soft Matter* **6** 739–42
[124] Kolesky D B, Truby R L, Gladman A S, Busbee T A, Homan K A and Lewis J A 2014 *Adv. Mater.* **26** 3124–30
[125] Kam D H and Mazumder J 2008 *J. Laser Appl.* **20** 185–91
[126] Grigoryan B *et al* 2019 *Science* **364** 458–64
[127] Huang J H, Kim J, Agrawal N, Sudarsan A P, Maxim J E, Jayaraman A and Ugaz V M 2009 *Adv. Mater.* **21** 3567–71
[128] Engelhardt S, Hoch E, Borchers K, Meyer W, Krüger H, Tovar G and Gillner A 2011 *Biofabrication* **3** 025003
[129] Arcaute K, Mann B K and Wicker R B 2006 *Ann. Biomed. Eng.* **34** 1429–41
[130] Schuster M, Turecek C, Kaiser B, Stampfl J, Liska R and Varga F 2007 *J. Macromol. Sci.* A **44** 547–57
[131] Baudis S, Nehl F, Ligon S C, Nigisch A, Bergmeister H, Bernhard D, Stampfl J and Liska R 2011 *Biomed. Mater.* **6** 055003
[132] Sarker M and Chen X B 2017 *J. Manuf. Sci. E-T ASME* **139** 081002
[133] Izadifar Z, Chang T, Kulyk W, Chen X and Eames B F 2016 *Tissue Eng.* C **22** 173–88
[134] You F, Wu X, Zhu N, Lei M, Eames B F and Chen X 2016 *ACS Biomater. Sci. Eng.* **2** 1200–10
[135] Kesari P, Xu T and Boland T 2005 *Nanoscale Mater. Sci. Biol. Med.* **6** 111–7
[136] Nakamura M, Nishiyama Y, Henmi C, Iwanaga S and Nakagawa H 2008 *J. Imaging Sci. Technol.* **52** 060201-1–060201-6
[137] Nakamura M, Nishiyama Y and Henmi C 2008 3D micro-fabrication by inkjet 3D biofabrication for 3D tissue engineering *IEE MHS 2008* pp 451–6
[138] Nishiyama Y, Nakamura M, Henmi C, Yamaguchi K, Mochizuki S, Nakagawa H and Takiura K 2009 *J. Biomech. Eng.* **131** 035001
[139] Xu C, Chai W, Huang Y and Markwald R R 2009 *Biotechnol. Bioeng.* **109** 3152–60
[140] Huber B, Borchers K, Tovar G E and Kluger P J 2016 *J. Biomater. Appl.* **30** 699–710
[141] Yanagawa F, Sugiura S and Kanamori T 2016 *Regen. Ther.* **3** 45–57 Special Issue: Hyper BioAssembler
[142] Bhattacharjee T, Zehnder S M, Rowe K G, Jain S, Nixon R M, Sawyer W G and Angelini T E 2015 *Sci. Adv.* **1** e1500655
[143] Zhang Y, Yu Y, Chen H and Ozbolat I T 2013 *Biofabrication* **5** 025004
[144] Zhang Y, Yu Y and Ozbolat I T 2013 *J. Nanotechnol. Eng. Med.* **4** 020902
[145] Luo Y, Lode A and Gelinsky M 2013 *Adv. Healthcare Mater.* **2** 777–83
[146] Jia W *et al* 2016 *Biomaterials* **106** 58–68
[147] Visser J, Peters B, Burger T J, Boomstra J, Dhert W J, Melchels F P and Malda J 2013 *Biofabrication* **5** 035007
[148] Skardal A, Zhang J, McCoard L, Xu X, Oottamasathien S and Prestwich G D 2010 *Adv. Mater.* **22** 4736–40
[149] Skardal A, Zhang J, McCoard L, Xu X, Oottamasathien S and Prestwich G D 2010 *Tissue Eng.* A **16** 2675–85
[150] Skardal A, Zhang J and Prestwich G D 2010 *Biomaterials* **31** 6173–81
[151] Sochi T 2015 *Int. J. Fluid Mech. Res.* **42** 59–81
[152] Simonelli M, Tse Y Y and Tuck C 2014 *Mater. Sci. Eng.* A **616** 1–11
[153] Yan X and Gu P 1996 *Comput. Aided Des.* **28** 307–18
[154] Quan Z, Wu A, Keefe M, Qin X, Yu J, Suhr J, Byun J H, Kim B S and Chou T W 2015 *Mater. Today* **18** 503–12
[155] Huang S H, Liu P and Mokasdar A 2013 *Int. J. Adv. Manuf. Technol.* **67** 1191–203
[156] Wong K V and Hernandez A 2012 *ISRN Mech. Eng.* **2012** 1–10
[157] Jacob G G K, Kai C C and Mei T 1999 *Comput. Ind.* **39** 61–70
[158] He Y, Xue G H and Fu J Z 2014 *Sci. Rep.* **4** 6973
[159] Chia H N and Wu B M 2015 *J. Biol. Eng.* **9** 4